to metabolic properties for human CYP2C19 (Matsunaga et al., 2002).

The monkey, the animal evolutionarily close to humans, shows not only phenotypic but also physiological similarities to humans in such biological circumstances as aging (Roth et al., 2004), reproduction (Bellino and Wise, 2003), and neurological disease, including Parkinson's disease (Takagi et al., 2005). This resemblance can be partly explained by a relatively high similarity (~97%) of protein sequences generally seen between monkeys and humans (Magness et al., 2005). For preclinical trials during drug development, monkeys, especially macaques, are used as a large and nonrodent species to evaluate drug effects because they generally show pharmacokinetics more similar to humans than any nonprimate models. However, it has become apparent that monkeys are not always similar to humans in drug metabolism (Stevens et al., 1993; Sharer et al., 1995; Guengerich, 1997; Weaver et al., 1999; Bogaards et al., 2000; Narimatsu et al., 2000). We hypothesized that this species difference was due to the difference in the genetic components essential for drug metabolism such as P450s between monkeys and humans. In monkeys, information on the characteristics of drug-metabolizing enzymes is largely scarce, especially at molecular level, preventing a deep understanding of drug metabolism. Therefore, to test our hypothesis, we have identified a number of the cynomolgus monkey cDNA clones for P450s; the characterization of these clones is currently ongoing. Successful drug development requires accuracy in the extrapolation of drug metabolism and toxicity data from experimental animals to humans. Then characterization of these cynomolgus P450s should help to better understand drug metabolism in monkeys.

In this article, we report the isolation and characterization of cynomolgus CYP2C76, a novel P450 with a low homology to any human or monkey CYP2C cDNAs. RT-PCR and immunoblotting indicated the expression of mRNA and protein homologous to CYP2C76 in cynomolgus and rhesus monkeys but not in humans. Moreover, the genomic analysis indicated that the *CYP2C76* gene was located at the end of the *CYP2C* cluster in the macaque genome, the location of which corresponded to an intergenic region in the human genome, suggesting that the P450 homologous to CYP2C76 does not exist in humans. The hepatic expression of CYP2C76 was higher than any other CYP2Cs analyzed, indicating that this P450 was a major CYP2C in the monkey liver. CYP2C76 protein was active in the metabolism of tolbutamide and testosterone. Because of its species specificity and functional importance, CYP2C76 might account for the species difference occasionally seen in drug metabolism between monkeys and humans.

Materials and Methods

Chemicals and Reagents. 4-Hydroxytolbutamide, 6α-hydroxypaclitaxel, 3-hydroxypaclitaxel, 4-hydroxy-*S*-mephenytoin, and 6β-hydroxytestosterone were purchased from Ultrafine Chemicals (Manchester, UK). Pooled hepatic microsomes from human subjects and male cynomolgus monkeys were both purchased from BD Gentest (Woburn, MA). Labeled [2-benzoyl ring-U-^{14}C]paclitaxel (2.23 MBq/mg) was obtained from Sigma-Aldrich (St. Louis, MO), whereas [ring-U-^{14}C]tolbutamide (2.26 GBq/mmol), *S*-[4-^{14}C]mephenytoin (9.42 MBq/mg), and [4-^{14}C]testosterone (2.11 GBq/mmol) were from GE Healthcare (Little Chalfont, Buckinghamshire, UK). The radiochemical purities of these ^{14}C-labeled chemicals were >99%. Oligonucleotides were synthesized by Sigma-Genosys (Ishikari, Japan). All other reagents were purchased from Sigma-Aldrich unless otherwise specified.

Tissue Samples and RNA Extraction. Tissue samples were collected from individual monkeys, including six cynomolgus monkeys (three male and three female) and two male rhesus monkeys, which were kept under the established guidelines and standard procedures at Shin Nippon Biomedical Laboratories (Tokyo, Japan). The study was approved by the local ethics committee. The tissue samples from brain, lung, heart, liver, kidney, adrenal gland, small intestine, testis, ovary, and uterus were frozen in liquid nitrogen right after removal from animals to prevent potential RNA degradation. Orangutan and chimpanzee liver samples were kindly provided by GAIN (Great Ape Information Network, Japan). The frozen tissues were first ground with mortar and pestle and then processed in TRIzol (Invitrogen, Carlsbad, CA) with a Polytron homogenizer (Kinematica, Basel, Switzerland), followed by extraction of total RNA according to the manufacturer's instruction. After treatment with DNase I (Takara, Tokyo, Japan), the RNA was purified using GenElute Mammalian Total RNA Mini Kit (Sigma-Aldrich).

Cell Culture and RNA Extraction. COS1 cells from the American Type Culture Collection (Manassas, VA) was cultured as described previously (Saito et al., 2001). RNA extraction from the cell and the subsequent DNase I treatment were performed using RNeasy Mini Kit (QIAGEN, Valencia, CA) according to the manufacturer's protocol.

Cloning of CYP2C76 Homologous cDNA in Other Primate Species. RNA was extracted from liver (for rhesus monkey, orangutan, and chimpanzee) and COS1 cell (for African green monkey). The first-strand cDNA was generated in a mixture containing 1 μg of total RNA, oligo (dT) or random primers, and Moloney murine leukemia virus reverse transcriptase (Toyobo, Osaka, Japan) at 37°C for 1 h. The resultant cDNA was diluted 25-fold and used as a template for the subsequent PCR. For human cDNA, the liver cDNA available from BD Biosciences (San Jose, CA) was used. The amplification was carried out using KOD Plus DNA polymerase (Toyobo) according to the manufacturer's protocol with the MJ Research thermal cycler (MJ Research, Watertown, CA). PCR conditions include an initial denaturation at 95°C for 2 min and 30 cycles of 95°C for 20 s, 55°C for 20 s, and 72°C for 2 min, followed by a final extension at 72°C for 10 min. Among several different primer-pairs tested, a CYP2C76 homologous sequence for rhesus and African green monkeys was successfully amplified by PCR using the following primer pairs: mf27B9 (5rt2), 5′-CCCAGCAATGGATCTCTTCA-3′, and mf27B9 (3polyA2a), 5′-TGCCTAGACAGGTAGATAGGAGTG-3′, for the rhesus monkey; mf27B9 (5rt2) and mf27B9 (3ex4b), 5′-GAAAAGTGGGATCACAGGGA-3′, for the African green monkey. After the addition of 3′ A-overhangs, the PCR products were cloned into vectors using TOPO TA Cloning Kit (Invitrogen). The inserts were then sequenced using ABI Prism BigDye Terminator v3.0 Ready Reaction Cycle Sequencing Kit (Applied Biosystems, Foster City, CA), followed by electrophoresis with the ABI Prism 3730 DNA Analyzer (Applied Biosystems).

Sequence Analysis. Raw sequence data were imported into DNASIS Pro (Hitachi Software, Tokyo, Japan) for most sequence analyses. After vector sequences and regions of sequence with unacceptable quality were removed, the trimmed sequences were assembled to the full-length sequence. A homology search was conducted by the BLAST program (National Center for Biotechnology Information). Multiple alignment of amino acid sequences was performed with the ClustalW program; the resultant alignment was used to create a phylogenetic tree using the PHYLIP program by default parameter. The human and chimpanzee genome data were searched for the sequence homologous to CYP2C76 by BLAT search (UCSC Genome Bioinformatics). Likewise, the macaque genome data (Baylor College of Medicine Human Genome Sequencing Center) were

used to identify and analyze the genome sequences corresponding to macaque CYP2Cs.

Amplification of CYP2C76 Introns. All the introns were amplified from cynomolgus monkey genomic DNA by PCR with 5 pmol each of forward and reverse gene-specific primers, 0.5 mM dNTPs, 2 mM $MgCl_2$, and 1 unit of LA *Taq* polymerase (Takara) in a total volume of 20 μl. The primers used to amplify introns 1 to 8 were mf27B9 (5rt2), mf27B9 (5ex2a), mf27B9 (5ex3a), mf27B9 (5ex4a), mf27B9 (5ex5a), mf27B9 (5ex6a), mf27B9 (5qrt1), or mf27B9 (5gen1) as a forward primer and mf27B9 (3ex2a), mf27B9 (3ex3a), mf27B9 (3ex4a), mf27B9 (3ex5a), mf27B9 (3ex6a), mf27B9 (3ex7a), mf27B9 (3qrt1), or mf27B9 (3rt1) as a reverse primer, respectively. The nucleotide sequence for each primer is listed below. Thermal cycler conditions were as follows: 95°C for 2 min; 35 cycles of 95°C for 20 s, 55°C for 30 s, and 72°C for 5 min; and a final extension at 72°C for 20 min. After electrophoresis in 0.8% agarose gels, the PCR products were gel-purified, cloned into vectors using TOPO XL Cloning Kit (Invitrogen), and sequenced. Sequencing and sequence analysis were performed as described above to determine the entire sequence of each intron.

The sequences of oligonucleotide primers used are as follows: mf27B9 (5ex2a), 5′-GTATTTTCTGGCCGAGGGAG-3′; mf27B9 (5ex3a), 5′-CGGCGTTTCTCTCTCATGGT-3′; mf27B9 (5ex4a), 5′-GGGTTGTGTTCCCTGTAATGTC-3′; mf27B9 (5ex5a), 5′-CATCAGGAATCTCTGGACATC-3′; mf27B9 (5ex6a), 5′-CAGAGACAACAAGCACCACAA-3′; mf27B9 (5qrt1), 5′-CCCATGCAGTGACTCAAGAC-3′; mf27B9 (5gen1), 5′-GCCACTTCCTGGACGAAAG-3′; mf27B9 (3ex2a), 5′-CTCCCTCGGCCAGAAAATAC-3′; mf27B9 (3ex3a), 5′-ATGCTTCCACCAGACACAAG-3′; mf27B9 (3ex4a), 5′-ACAGGGAACACAACCCAGAA-3′; mf27B9 (3ex5a), 5′-CGAGGGTTATTGATGTCCAGAG-3′; mf27B9 (3ex6a), 5′-GGAGCATCAGTCCATATCTCATT-3′; mf27B9 (3ex7a), 5′-ATTGGTGGGGATGAGGTCAATA-3′; mf27B9 (3qrt1), 5′-AAGTGGCCAGGGTCAAACT-3′; and mf27B9 (3rt1), 5′-ACAGCCTTGCTCTGCAATC-3′.

Isolation and Analysis of Monkey BAC Clones. The BAC clone containing the *CYP2C* genes was isolated by screening a rhesus monkey BAC library (BACPAC, Oakland, CA) using the CYP2C75 and CYP2C76 cDNAs as probes, because the BAC library was not available for cynomolgus monkeys. Hybridization with the library filters was carried out as recommended by the manufacturer using the probes synthesized in the presence of [α-^{32}P]dCTP (GE Healthcare) with the RadPrime DNA labeling system (Invitrogen). The identified BAC clones were obtained from the BACPAC. The BAC DNA was purified using DNA PhasePrep BAC DNA Kit (Sigma-Aldrich). To identify the *CYP2C* genes contained in each BAC DNA, the purified DNA was used as a template for the PCR with specific primers for 5′ or 3′ of each gene, 0.5 mM dNTPs, 2 mM MgCl2, and 1 unit of AmpliTaq Gold DNA polymerase (Applied Biosystems) in a total volume of 20 μl. PCR conditions were as follows: 95°C for 10 min; 30 cycles of 95°C for 20 s, 55°C for 20 s, and 72°C for 1 min; and final extension at 72°C for 10 min. The different primer pairs were initially designed at exons 1 and 9 of each gene, the location of which was determined by comparing each cynomolgus cDNA to the human *CYP2C* genes. For the genes highly homologous to *CYP2C43* and *CYP2C75*, the designed primers did not show a gene-specific amplification pattern. Therefore, the gene-specific indels were identified in introns 1 and 8 of these genes by searching the macaque genome data and the primers recognizing these indels were designed. The sequences of primers used for the PCR are listed in Table 1. The amplification pattern was examined to determine an arrangement of the *CYP2C* genes in the genome as described previously (Gray et al., 1995). For the same purpose, the DNA was also used for the BAC end sequencing and for a restriction enzyme mapping with BamHI or EcoRI as recommended by the BACPAC.

Real-Time RT-PCR. The primers and TaqMan MGB probes specific for each gene (Table 2) were designed using Primer Express software (Applied Biosystems). The 5′ end of the probes was labeled with 5-carboxyfluorescein fluorescence reporter dye. Reverse transcriptase reaction was carried out using random primers as described above. A twenty-fifth volume of the reaction mixture was then used for the subsequent PCR that was carried out in a total volume of 25 μl using TaqMan Universal PCR Master Mix (Applied Biosystems) with the ABI Prism 7700 sequence detection system (Applied Biosystems) following the manufacturer's protocol. Final concentration of each primer set was 0.3 μM for CYP2C20 and CYP2C43, 0.9 μM for CYP2C75, and 0.1 μM for CYP2C76. The final concentration of the probes was 0.25 μM for all CYP2Cs. Thermal cycler conditions for all reactions were 2 min at 50°C and 10 min at 95°C, followed by 40 cycles of 15 s at 95°C and 1 min at 60°C. Standard curves were generated by serial 10-fold dilutions of a plasmid for the corresponding cDNA. The specificity of assays for all *CYP2C* genes was confirmed by sequencing a single DNA band with the expected size in agarose gels and by performing the highly efficient amplification of cDNA plasmid for the target gene over that of the other *CYP2C* genes. Relative expression level of each gene was normalized to the 18S ribosomal RNA level measured using a predeveloped kit available from Applied Biosystems. At least three amplifications were performed for each gene.

Heterologous Expression of Four Recombinant CYP2Cs in *Escherichia coli*. Protein expression of the four CYP2Cs was carried out as described previously (Iwata et al., 1998). To enhance protein expression, the eight residues of the N terminus were replaced with the corresponding ones of the modified bovine CYP17, MALLLAVF (Barnes et al., 1991) by amplifying the open reading frame of each cDNA with the primers listed in Table 3 using the KOD Plus DNA polymerase. The forward and reverse primers contained

TABLE 1
Primers used for amplification of *CYP2C*-positive BAC clones

Gene	Sequence (5′→3′)	
	Forward	Reverse
CYP2C20		
5′	ATGGAACCTTTTGTGGTCCTG	GAAAGATTTGCAGATGTCCTTAAC
3′	TTTGTGCAGGAGAGGGACTT	ACGAGGGTGGCAGAGAAAT
CYP2C43		
5′	TCTTGAAGCTGGGTATTGGTC	AGGTGGATCACAAGGTCAGG
3′	GGATAAAATTATCCTCAAAATCCTC	CATCAAAGGTCACAGAATAAAGG
CYP2C75		
5′	TTGTTGCCTTTTCTCCATCA	CACGGTTAAACCATCTTTCACA
3′	GTTAAAGGAGATAATGAGCCACAG	GGAAAGATGTGTTTGCTTCCAC
CYP2C18-like		
5′	GTGAAAGCCCACAGTTTTCTTAC	CTCATGTCCTTAACATCTAACTGC
3′	TGACATCACCCCCATTGC	TGTGGGTTGACAAGTCAGAG
CYP2C76		
5′	CCCAGCAATGGATCTCTTCA	TGGCACCAAGCATTTATCTC
3′	CTTGCCTGTGTGTCAACCAT	ATTGGAATGGATTTTGAAGGA

NdeI and XbaI sites, respectively, so that after restriction enzyme digestion, the PCR products can be easily cloned into the pCW vector (Barnes, 1996), in which the human reductase cDNA has been already accommodated (Iwata et al., 1998). The resultant construct for CYP2C20, CYP2C43, CYP2C75, or CYP2C76 was used to transform DH5α competent cells (Invitrogen). Thereafter, sequence and orientation of each insert were confirmed by sequencing. To express proteins, the bacteria cells grown overnight in Luria-Bertani broth were diluted 100-fold and cultured in the presence of 200 μg/ml ampicillin for 6 to 12 h at 30°C in the modified Terrific broth (Iwata et al., 1998) until the optical density at 600 nm reached approximately 0.6 to 0.8. Isopropyl-β-D-thiogalactoside was then added to the culture at a final concentration of 1.5 mM. After 16 to 20 h, the cultured cells were harvested and cell membrane fraction was prepared as described previously (Daigo et al., 2002). The content of each CYP2C protein in the membrane preparation was determined by $Fe^{2+} \cdot CO$ versus Fe^{2+} difference spectra, according to the method described by Omura and Sato (1964) using the U-3000 spectrophotometer (Shimadzu, Kyoto, Japan). The concentration of NAPDH-P450 reductase was also measured as reported previously (Iwata et al., 1998; Daigo et al., 2002).

Drug-Metabolizing Activity of the Partially Purified Preparations of Monkey CYP2Cs. All the recombinant CYP2C proteins were analyzed for their activities to metabolize drugs with four substrates prototypical for human P450s, including paclitaxel, tolbutamide, *S*-mephenytoin, and testosterone. To prepare the reaction mixture, [^{14}C]paclitaxel (6 μM), [^{14}C]tolbutamide (100 μM), [^{14}C]*S*-mephenytoin (50 μM), or [^{14}C]testosterone (50 μM) was preincubated in a 100 mM sodium phosphate buffer solution, pH 7.4, with hepatic microsomes (1 mg/ml) or the partially purified recombinant CYP2Cs (200 pmol/ml) at 37°C for 5 min. This was followed by the addition of a NADPH regenerating system containing 1.3 mM $NADP^+$, 3.3 mM glucose 6-phosphate, 0.4 U/ml glucose-6-phosphate dehydrogenase, and 3.3 mM magnesium chloride in 100 mM sodium phosphate buffer, pH 7.4, so that the metabolic reaction was initiated at a final concentration of 1 mg of protein/ml or 200 pmol of P450/ml. After incubation at 37°C for 15 min (paclitaxel and testosterone), 45 min (*S*-mephenytoin), or 60 min (tolbutamide), the reaction was quenched by adding an equal volume of 100% methanol solution. For the recombinant CYP2Cs, the incubation was carried out for 30 min with all the tested substrates. The reaction-terminated samples were centrifuged, the aliquots of the supernatant were evaporated to dryness, and the residue was dissolved in 15 μl of methanol. The analysis of 6α-hydroxypaclitaxel and 3-hydroxypaclitaxel was performed as reported previously (Fujino et al., 2001). Aliquots (~2 μl) of the supernatant were spotted onto TLC plates (Silicagel 60F254, 20 × 20 cm; Merck, Darmstadt, Germany) and developed with toluene-acetone-formic acid [60:39:1 (v/v/v)] to 12 cm in a horizontal TLC chamber that was saturated with solvent vapor. The analysis of 6β-hydroxytestosterone was carried out as follows: supernatant was applied to TLC plates and developed with dichloromethane-acetone [4:1 (v/v)] to 16 cm. The measurement of 4-hydroxytolbutamide was performed as reported previously (Ludwig et al., 1998). In brief, the supernatant was spotted and developed with toluene-acetone-formic acid [60:39:1 (v/v/v)] to 10 cm. The assay for *S*-mephenytoin 4-hydroxylase activity was also performed according to a previous report (Shimada et al., 1985). The spotted supernatant was developed with chloroform-methanol-28% ammonium [90:10:1 (v/v/v)] to 12 cm. The TLC plates were dried and placed in contact with a phosphor imaging plate for 12 h. The amounts of unchanged drug and metabolites were determined using the BAS-2500 (Fuji Photo Film Co., Tokyo, Japan). The radioactive metabolites were positively identified by a comparison of R_f values using authentic unlabeled standard.

Immunoblotting. Polyclonal antibodies raised to CYP2C76 were produced by NeoMPS (San Diego, CA) using specific peptides for this protein. In brief, a peptide specific for CYP2C76 (Fig. 1) was designed, synthesized, purified, coupled through the terminal cysteine thiol with a keyhole limpet hemocyanin, and used to immunize New Zealand white rabbits. The recombinant P450 proteins (1.0 pmol each) were run in 10% SDS polyacrylamide gels and transferred to Hybond-P filters (GE Healthcare). The filters were immunoblotted with the rabbit anti-CYP2C76 (1:250) and the donkey anti-rabbit IgG conjugated with horseradish peroxidase (SantaCruz Biotechnology, Santa Cruz, CA). To detect protein disulfide isomerase (PDI) as a loading control, rabbit anti-PDI (1:200, SantaCruz Biotechnology) was also used. A specific band was visualized using an ECL Western blotting detection reagent (GE Healthcare) according to the manufacturer's instructions.

Immunohistochemistry. The sections of cynomolgus monkey liver were immunostained with the anti-CYP2C76 antibody after the standard procedure. In brief, the primary antibodies were diluted 50-fold and applied to the sections at 4°C overnight. The bound antibodies were detected using the EnVision+ System (Dako North America, Inc., Carpinteria, CA) and liquid diaminobenzidine (Dako North America) according to the manufacturer's instruction. Slides were counterstained with Harris hematoxylin. As a negative control, rabbit preimmune serum was used instead of primary antibodies. To validate immunohistochemical specificity, the antibodies were preincubated at 4°C overnight with excess amount of the CYP2C76

TABLE 2
Primers and probes used for real-time RT-PCR

Gene and Primer/Probe	Sequence (5′ → 3′)
CYP2C20	
Forward	TTTCTGGAAGAGGCATTTTGC
Reverse	TCCATCTCTTTCCATTGCTGG
Probe	AACGGACTTGGAATCA
CYP2C43	
Forward	GCCATTTCCCACTGTTTGAAA
Reverse	GCAGCGTCATGAGGGAGAA
Probe	ACAATTCCAAATCTTCT
CYP2C75	
Forward	TTCCATTGGCTGACAGAGCTAA
Reverse	CCGCAGTGTCATGAGGGAA
Probe	CGATTCCAAATCCT
CYP2C76	
Forward	TGGCCGAGGGAGTTTTCC
Reverse	AGAGAGAAACGCCGAATTTGC
Probe	CCAAGGATTCGGAGTTA

TABLE 3
Primers used to construct plasmids for protein expression
Bold letters show the modified N-terminal sequence, and underline indicates the NdeI or XbaI restriction site for forward or reverse primers, respectively.

cDNA and Direction	Sequence (5′ → 3′)
CYP2C20	
Forward	GGAATTCCATATGGCTCTGTTATTAGCAGTTTTTCTCTGTCTCTCCTTTGTGC
Reverse	GCTCTAGACAGATGGGCTAGCATTCTTCA
CYP2C43/CYP2C75	
Forward	GGAATTCCATATGGCTCTGTTATTAGCAGTTTTTCTCTGTCTCTCCTGTTTGC
Reverse	GCTCTAGACCAGACCATCTGCTCTTCTT
CYP2C76	
Forward	GGAATTCCATATGGCTCTGTTATTAGCAGTTTTTATTTGTCTTTCTTGTCTGAT
Reverse	GCTCTAGACTAGCAGCCAGACACTTCA

specific peptide (0.05 mg/ml) and this mixture was used in place of primary antibodies for immunohistochemistry.

Results

Identification of Cynomolgus CYP2C cDNAs. CYP2C76, along with CYP2C20, CYP2C43, and CYP2C75, was originally identified as a unique cDNA clone by searching our in-house EST database that was established using a full-length cDNA library prepared from the cynomolgus monkey liver (Y. Uno, Y. Suzuki, Y. Sakamoto, H. Sano, K. Hashimoto, S. Sugano, and I. Inoue, unpublished data). Among these, the se-quences newly identified in cynomolgus monkey, CYP2C43, CYP2C75, and CYP2C76, have been deposited to GenBank under accession numbers of DQ074806, DQ074805, and DQ074807, respectively. The CYP2C76 cDNA contained the open reading frame of 489 amino acids (Fig. 1). The deduced amino acid sequence showed primary sequence structures common to CYP2C molecules, including a highly hydrophobic N terminus, heme-binding region, and six potential substrate recognition sites (Gotoh, 1992). Blast analysis using the deduced amino acid sequences showed that CYP2C76 had only ~71% identity to any human CYP2Cs, whereas CYP2C20, CYP2C43, and CYP2C75 were ~92% homologous to human CYP2C (Table 4). This, together with a phylogenetic comparison of CYP2C amino acid sequences among mammalian species (Fig. 2), indicated possibilities that the CYP2C76 might be monkey-specific or that the human ortholog has not been isolated. To examine the latter possibility, we attempted to identify the sequence homologous to CYP2C76 in humans and other primate species by RT-PCR using gene-specific primer pairs. RNA samples used were from humans, the great apes (chimpanzee and orangutan), and Old World monkeys (cynomolgus, rhesus, and African green monkeys). The amplification was seen for Old World monkeys, and sequences of the PCR products were determined (data not shown). These CYP2C76 homologous sequences were ≥99% identical to each other, reflecting evolutionary closeness of these species. In contrast, the amplification with the human, chimpanzee, and orangutan samples showed no detectable bands in agarose gels (data not shown). Moreover, searching human and chimpanzee genome databases by BLAT (UCSC Genome Bioinformatics) showed no potential *CYP2C* genome sequence ≥90% homologous to the *CYP2C76*, raising the possibility that the CYP2C76 is monkey-specific.

Genomic Organization of the Monkey *CYP2C* Locus. To confirm the species specificity for CYP2C76, the location of the *CYP2C76* in the genome was determined by analyzing rhesus monkey CYP2C BAC clones. The *CYP2C*-positive clone was used for PCR as a template with gene-specific primers that were assigned at the 5′ and 3′ ends of each cynomolgus CYP2C cDNA. During the course of this study, the genome sequence data of the rhesus monkey became available and was used to confirm that the designed primers could be used for the rhesus monkey. The analysis of the data identified the genome sequence highly homologous to human *CYP2C18*. Therefore, the primers specific for this *CYP2C18*-like gene were also designed and used for amplification with the BAC clones. The amplification pattern of each gene, together with the end-sequencing and the restriction enzyme mapping of the BAC clones, indicated that the five *CYP2C*

TABLE 4
Amino acid identity among human and monkey CYP2Cs

	CYP2C20	CYP2C43	CYP2C75	CYP2C76
			%	
CYP2C8	92	78	76	70
CYP2C9	78	93	93	71
CYP2C18	77	81	81	72
CYP2C19	79	91	92	72
CYP2C20		78	77	70
CYP2C43			94	71
CYP2C75				71

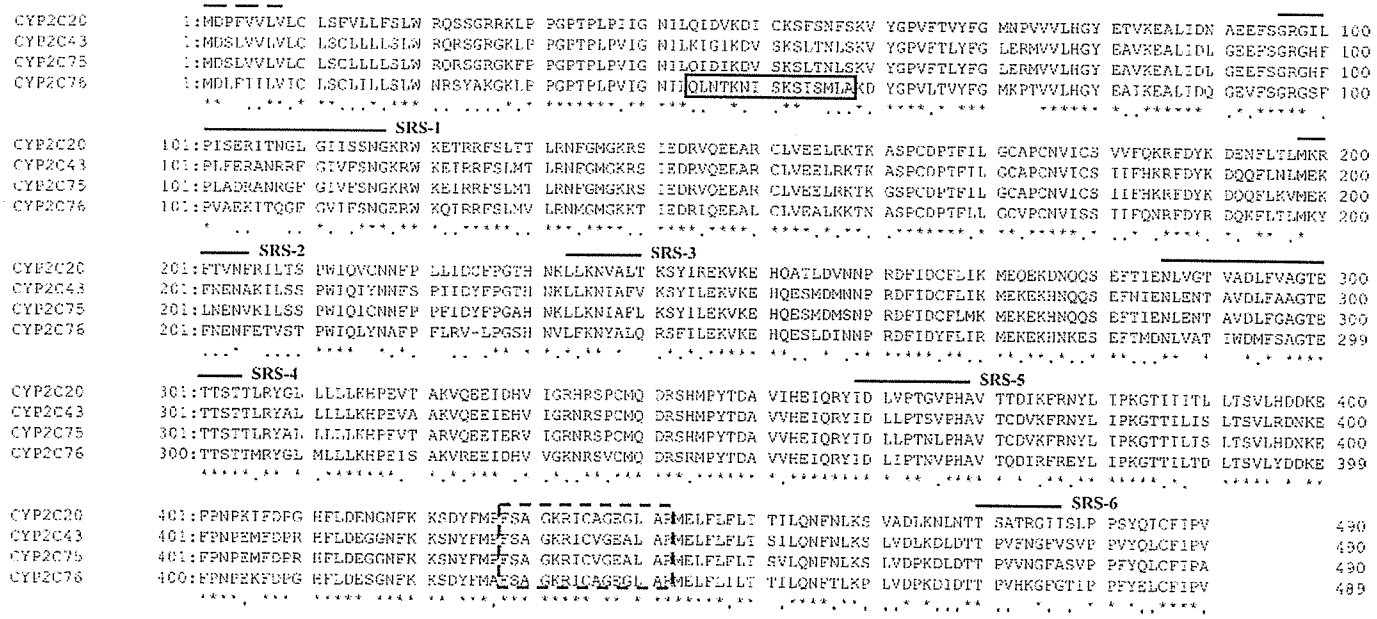

Fig. 1. Multiple alignment of amino acid sequences deduced from cynomolgus monkey CYP2C cDNAs. The putative heme-binding region characteristic of P450 protein is boxed with broken line. The broken and solid lines above the sequences indicate regions modified for protein expression and the six putative substrate recognition sites, respectively. The location of the peptide sequences used to raise the anti-CYP2C76 antibodies is boxed with solid line. Asterisks and dots under the sequences indicate identical amino acids and conservatively changed amino acids, respectively.

genes together form a gene cluster in the monkey genome similar to humans (Fig. 3). Moreover, *CYP2C76* was located at the end of the cluster, corresponding to the intergenic region adjacent to the *CYP2C* cluster in the human genome. These results strongly support the idea that *CYP2C76* is expressed in monkeys but not in humans.

Gene Structure of *CYP2C76*. To determine the gene structure of *CYP2C76*, long PCR amplification was performed with the genomic DNA of cynomolgus monkey as a template. Gene-specific primers were designed on each exon to amplify each intron. The sequences of the PCR products were determined as described above and assembled into the

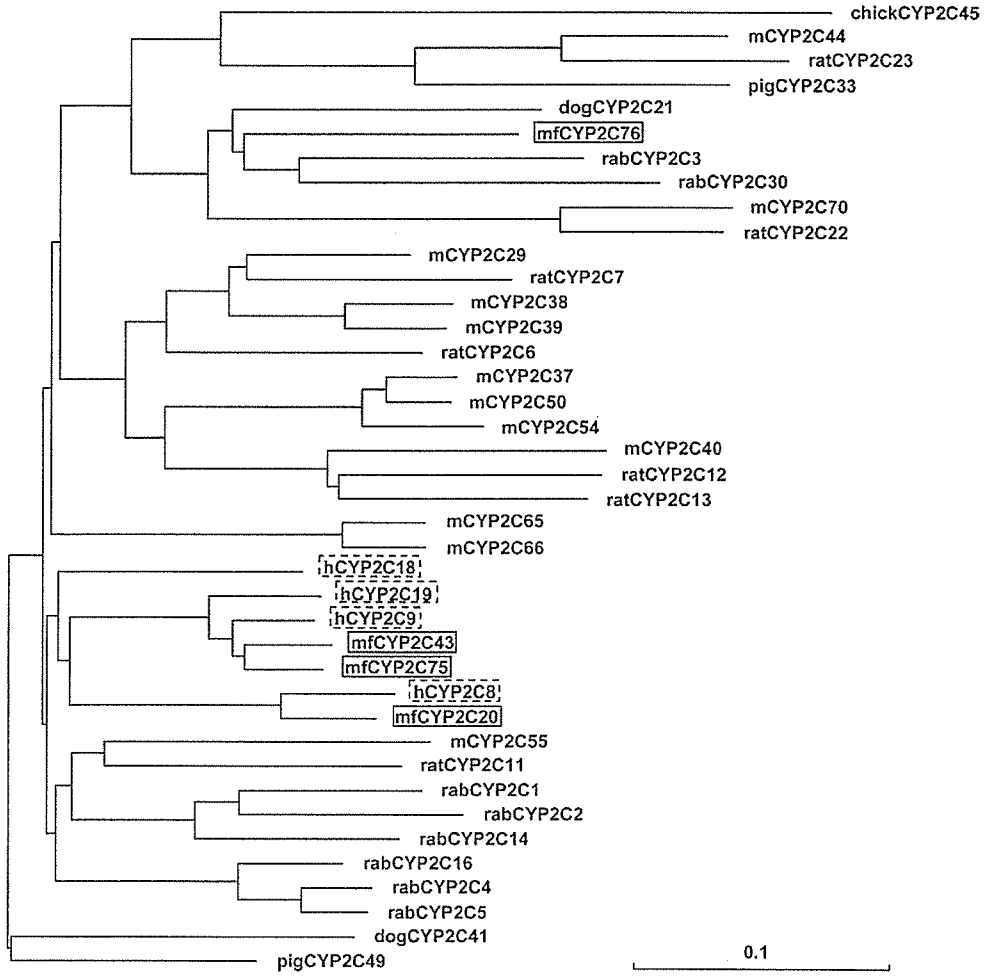

Fig. 2. Phylogeny of CYP2C amino acid sequences from cynomolgus monkey and other animal species. The phylogenetic tree was created using the Clustral W program. CYP2C amino acid sequences used were from cynomolgus monkey (mf), human (h), pig, dog, rabbit (rab), rat, mouse (m), and chicken (chick). The monkey and human CYP2Cs are boxed using solid and broken lines, respectively.

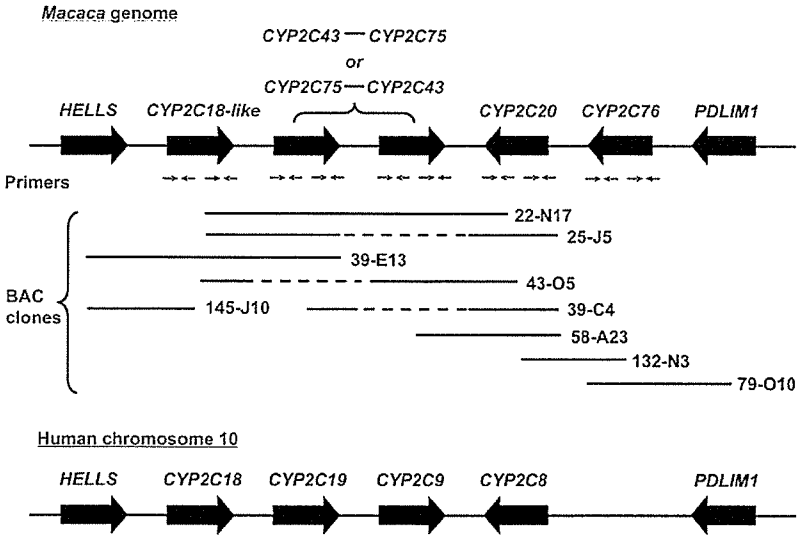

Fig. 3. Genomic structure of the monkey *CYP2C* genes. The *CYP2C* genes form the gene cluster in the macaque genome similar to the human genes as determined by PCR amplification patterns, and restriction enzyme mapping and end-sequencing of the *CYP2C*-positive BAC clones. Because an inter-relationship between *CYP2C43* and *CYP2C75* in the genome could not been clearly determined because of a high sequence homology of the two genes, the figure shows a tentative order of these genes. The broken lines indicate the regions of the BAC clones without a clear amplification, probably because of mispriming of the primers used.

entire intron. The *CYP2C76* gene spanned approximately 19.6 kb and contained nine exons, as has been described for all human *CYP2C* genes. Sizes of exons and introns ranged from 142 to 693 base pairs and from 937 to 4307 base pairs, respectively (Table 5). All exons were flanked by GU and AG dinucleotides consistent with the consensus sequences for splice junctions in eukaryotic genes, with the exception of the 5′ splice site for intron 8, where GU was replaced by GC.

Tissue Distribution of Gene Expression. To analyze the expression of cynomolgus *CYP2C20*, *CYP2C43*, *CYP2C75*, and *CYP2C76*, real-time RT-PCR was performed with gene-specific primers and TaqMan MGB probes using RNAs prepared from brain, lung, heart, liver, kidney, adrenal gland, small intestine, testis, ovary, and uterus. All the four *CYP2C* genes were expressed predominantly in the liver with some extrahepatic expression (Fig. 4). Among these CYP2Cs, the expression level of *CYP2C76* was the highest, indicating that CYP2C76 is a major CYP2C in the monkey liver.

Drug-Metabolizing Activities of Monkey Recombinant CYP2Cs. The activity of monkey CYP2Cs to metabolize drugs was characterized by incubating partially purified recombinant CYP2Cs with NADPH-regenerating system in the presence of the radiolabeled substrates typical for human CYP2Cs, paclitaxel, tolbutamide, *S*-mephenytoin, and testosterone. The results showed that CYP2C20 was involved only in the metabolism of paclitaxel among the four substrates examined, similar to the metabolic properties observed for human CYP2C8 (Fig. 5A). Tolbutamide was metabolized by CYP2C75 and CYP2C76 (Fig. 5B), whereas *S*-mephenytoin was only weakly metabolized by CYP2C43 and CYP2C75 (Fig. 5C). Testosterone was efficiently metabolized by all the four CYP2Cs except for CYP2C20, in which the metabolites generated were different (Fig. 5D). It is noteworthy that all three P450s capable of metabolizing testosterone generated one common but unknown metabolite. In addition, the 6β-hydroxylation of testosterone and the 3-hydroxylation of paclitaxel, both of which are mediated by CYP3A4 in humans, were not observed in the presence of CYP2Cs. Our results indicate that each monkey CYP2C has the characteristic substrate specificity.

Immunoblotting and Immunohistochemistry. The peptide specific for CYP2C76 was synthesized and used to raise anti-CYP2C76 antibodies. To investigate the specificity of the antibodies, immunoblotting was performed using the recombinant proteins, including monkey CYP2C20, CYP2C43, CYP2C75, and CYP2C76, in addition to human CYP2C8, CYP2C9, CYP2C18, and CYP2C19. Among these proteins, the antibodies detected a single ~50-kDa band only in CYP2C76 (Fig. 6A), indicating the immunospecificity of the antibodies. The immunoblotting for CYP2C76 was also carried out with liver microsomes prepared from five primate species: human, chimpanzee, orangutan, and cynomolgus and rhesus monkeys. A signal of the expected size was clearly detected only with liver microsomes from cynomolgus and rhesus monkeys (Fig. 6B), coincided well with the results of the gene expression pattern of *CYP2C76*.

To determine the cellular localization of the CYP2C76 protein, the cryosections prepared from the cynomolgus monkey liver were stained with the anti-CYP2C76 antibodies. Strong staining was seen in the cytoplasm of hepatocytes but not in the cells lining the bile duct or the vein (Fig. 7A). Little or no staining was seen after peptide blocking (Fig. 7B) or with preimmune serum (Fig. 7C), indicating that the staining was specific for CYP2C76.

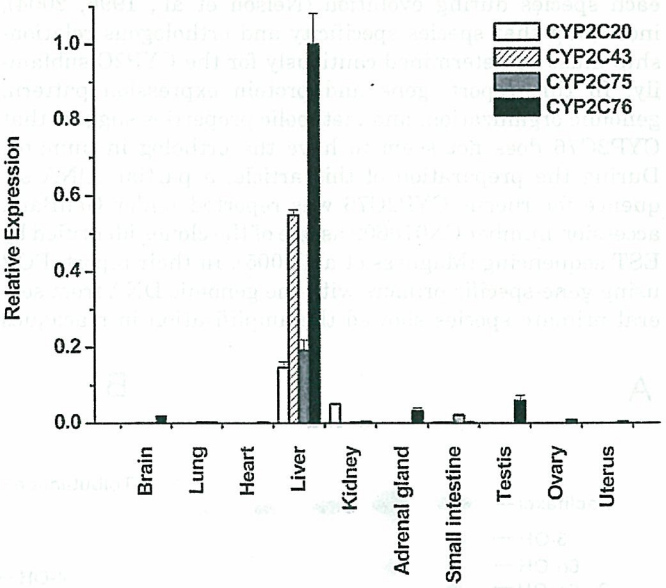

Fig. 4. Tissue distribution of *CYP2C* gene expressions in cynomolgus monkeys. Real-time RT-PCR was performed with each probe and primer set specific for *CYP2C20*, *CYP2C43*, *CYP2C75*, and *CYP2C76* using the RT products generated from total RNA of ten tissues. Expression level of each *CYP2C* gene was normalized to 18S rRNA level and represents the average ± S.D. from at least three independent experiments. For graphic representation, the expression level of *CYP2C76* for liver was adjusted to 1, and all other values were compared with the CYP2C76 level in liver.

TABLE 5
Sequences at each exon-intron boundary of *CYP2C76*
Exon and intron sequences are indicated in small and capital letters, respectively. The dinucleotide sequence at the highly conserved GU-AG motif is underlined.

Exon	Exon Size	3′ Splice Site	5′ Splice Site	Intron Size
	bp			*bp*
1	220		AAGCATG<u>gt</u>aagtatg	4148
2	163	ttttt<u>gc</u>agCTAGCAA	GGATTCG<u>gt</u>atgcttc	1436
3	150	tgttga<u>tag</u>GAGTTAT	ACCAATG<u>gt</u>gtttgtt	2221
4	161	tgtttg<u>tag</u>CATCTCC	GATACAG<u>gt</u>aaggcca	1259
5	173	tcctttc<u>ag</u>CTCTACA	GGAAAAG<u>gt</u>acaatgt	937
6	142	cattgct<u>ag</u>GAAAAAC	ATCTCAG<u>gt</u>atgatca	1046
7	188	ccttgcc<u>ag</u>CTAAAGT	TCCAAAG<u>gt</u>gagagat	4307
8	142	cttttt<u>ag</u>GGCACAA	TCAGCAG<u>gc</u>aagcaag	2172
9	≥693	aatttt<u>ag</u>GAAAAAG		

bp, base pairs.

Discussion

Monkeys have been employed in the preclinical studies of drug metabolism because they are believed to show a metabolic profile similar to that of humans. However, a different pattern is occasionally seen in drug metabolism between monkeys and humans (Stevens et al., 1993; Sharer et al., 1995; Guengerich, 1997; Weaver et al., 1999; Bogaards et al., 2000; Narimatsu et al., 2000). The molecular mechanism(s) behind this phenomenon remains unclear, partly as a result of the lack of detailed information on the genes and molecules responsible for drug metabolism in monkeys. In this study, to understand a possible cause responsible for this species difference, we identified a cDNA for CYP2C76 and characterized along with other CYP2C cDNAs encoding CYP2C20, CYP2C43, and CYP2C75 in cynomolgus monkeys. We investigated species specificity and tissue distribution of gene expression, in addition to genomic organization and metabolic properties.

The CYP2C subfamily has been known to be diverged in each species during evolution (Nelson et al., 1996, 2004), indicating that species specificity and orthologous relationship must be determined cautiously for the CYP2C subfamily. In this report, gene and protein expression pattern, genomic organization, and metabolic properties suggest that CYP2C76 does not seem to have the ortholog in humans. During the preparation of this article, a partial cDNA sequence for rhesus CYP2C76 was reported under GenBank accession number CX078602 as one of the clones identified by EST sequencing (Magness et al., 2005). In their report, PCR using gene-specific primers with the genomic DNA from several primate species showed the amplification in macaques but not in humans, further supporting our results. A definite conclusion could be made when a complete sequence of the monkey genome will be available.

The highly homologous *CYP2C* genes tend to be located near each other within the gene cluster, whereas *CYP2C44*, least homologous to other subfamily members, is located ~4 × 10^6 bases away from the mouse *CYP2C* gene cluster (Nelson et al., 2004). In contrast, *CYP2C76* (also least identical to any other *CYP2C* genes and thus placed outside the CYP2C group in the phylogenetic tree) is located within but on the edge of the *CYP2C* cluster in the monkey genome, similar to the mouse *CYP2C70* gene. The outer location probably did not allow *CYP2C76* for efficient crossover, resulting in the lower identity to other CYP2C subfamily members as has been proposed for *CYP2C44* and *CYP2C70* (Nelson et al., 2004). It is of great interest to know how *CYP2C76* has arisen after human and Old World monkeys diverged from a common ancestor around 25 million years ago (Kumar and Hedges 1998). Sequencing the *CYP2C* cluster of the closely related primate species should give an insight into this question.

Transcript variants influence the function of the P450 genes. Two transcript variants of *CYP4F3* contain either exon 3 or exon 4 generated through alternative splicing, leading to the high varieties of the synthesized proteins to accommodate different substrates as well as tissue specificity in gene expression (Christmas et al., 2001). In contrast, we identified a transcript variant for *CYP2C76* that lacks one of the exons, probably because of alternative splicing, which does not seem to have functional importance because of the premature termination codon (PTC) generated (data not

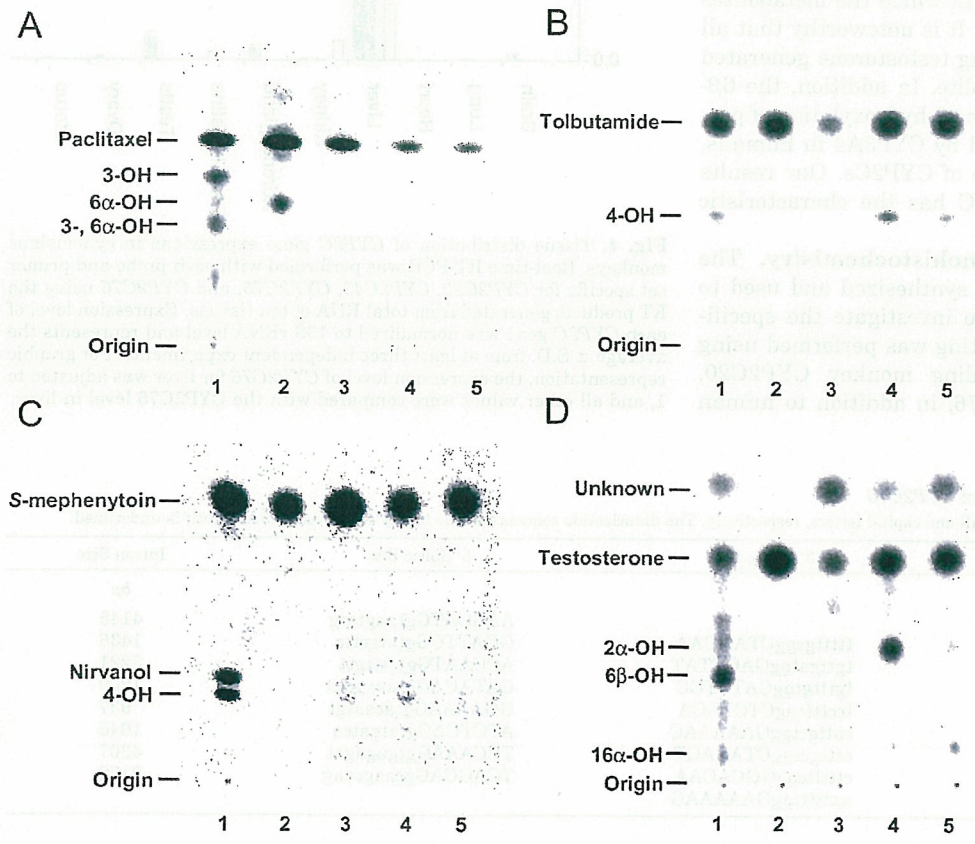

Fig. 5. High-performance liquid chromatography chromatograms after incubation of recombinant CYP2Cs with human CYP2C substrates. The reaction was performed using 1 mg/ml monkey hepatic microsomes or 200 pmol/ml the recombinant P450 in the presence of 6 μM paclitaxel (A), 100 μM tolbutamide (B), 50 μM *S*-mephenytoin (C), or 50 μM testosterone (D). The incubation time was 15 and 60 min for the microsomes and 30 min for the recombinants, respectively. Lanes 1 to 5 indicate the monkey hepatic microsomes, CYP2C20, CYP2C43, CYP2C75, and CYP2C76, respectively. Results are representative of three independent experiments.

shown). The PTC mRNAs can be subjected to a rapid degradation by nonsense-mediated decay (NMD) when PTCs are located more than 50 nucleotides before the last exon-exon junction (Holbrook et al., 2004). NMD is responsible for the degradation of the transcript variants generated by the *CYP3A5*3* allele, which can explain the difference in the expression levels of mRNAs between this and other genotype groups (Kuehl et al., 2001; Busi and Cresteil, 2005). Moreover, at least one third of alternative transcripts in humans were identified as PTC mRNAs, potential targets for RNA decay pathway through NMD (Lewis et al., 2003). Because gene expression is not completely diminished by NMD, expression levels remained would vary considerably between RNA isoforms, cell types, and even individuals (Holbrook et al., 2004). Therefore, together with the effect of SNPs on alternative splicing, the transcript variant of *CYP2C76* we identified, if subjected to NMD, could increase functional complexity of this gene.

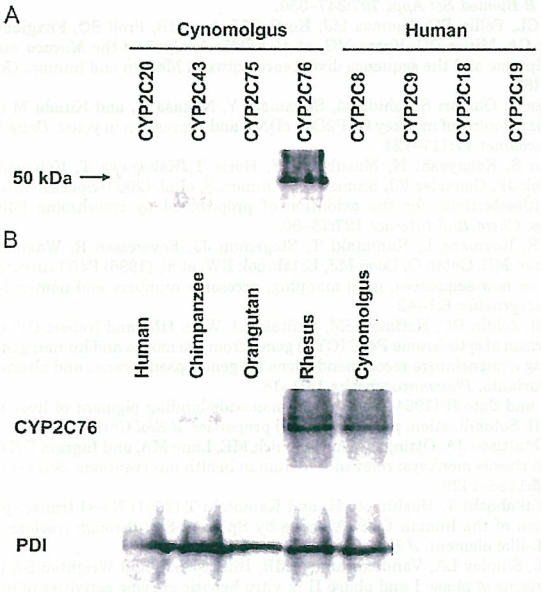

Fig. 6. Immunoblotting using the anti-CYP2C76 antibodies. The recombinant P450s (1.0 pmol of P450/lane) or liver microsomes (15 μg) were electrophoresed, transferred to polyvinylidene difluoride filters, and immunoblotted using anti-CYP2C76 antibodies. Each figure shows the representative image of three independent experiments. A, to investigate the specificity of the anti-CYP2C76 antibodies, the recombinant P450s were analyzed, including CYP2C20, CYP2C43, CYP2C75, and CYP2C76 for cynomolgus monkeys, and CYP2C8, CYP2C9, CYP2C18, and CYP2C19 for humans. B, to examine the presence of CYP2C76-homologous protein in other primate species, immunoblotting was performed with liver microsomes from humans, chimpanzee, orangutan, and rhesus and cynomolgus monkeys. PDI was used as a loading control.

CYP2C76 showed characteristic metabolic properties compared with CYP2C20, CYP2C43, and CYP2C75. CYP2C76 was critically involved in the metabolism of tolbutamide and testosterone, the metabolic properties of which are different from the other monkey CYP2Cs analyzed. CYP2C76, as a species-specific CYP2C enzyme, certainly adds the complexity to drug metabolism in monkeys and might account for the species difference in drug metabolism between monkeys and humans. Indeed, we have revealed that the CYP2C76 is at least partly responsible for the difference between monkeys and humans in the metabolism of a currently prescribed drug (Y. Uno, Y. Suzuki, Y. Sakamoto, H. Sano, K. Hashimoto, S. Sugano, and I. Inoue, unpublished observations). Further investigation of CYP2C76 on metabolic activity for a variety of substrates will help to better understand drug metabolism in monkeys and species difference between monkeys and humans.

The species difference of drug metabolism has been a major issue in drug development, because the results obtained with experimental animals need to be extrapolated to humans. The analysis for the capacity of hepatic microsomes from several animal species to metabolize drugs revealed that some differences occur in monkeys for the metabolism of marker substrates compared with humans (Sharer et al., 1995; Weaver et al., 1999; Bogaards et al., 2000). Tolbutamide hydroxylase activity is at least 3-fold lower in cynomolgus monkeys than humans (Sharer et al., 1995; Weaver et al., 1999), in contrary to our expectation because of monkey CYP2C75 and CYP2C76 exhibiting activities toward this substrate. This discrepancy might be due to the lower enzymatic activities of these enzymes compared with CYP2C9. However, other factors also need to be considered, such as genetic polymorphisms in individuals, from which the cDNA sequence used for protein expression was derived, because as in humans, monkeys have a diverse genetic background. Considering that even a single amino acid substitution can alter the enzymatic activity of P450s (Guengerich, 1997), nonsynonymous single nucleotide polymorphisms might have reduced the activity of CYP2C75 and CYP2C76. To examine this possibility, the genetic polymorphisms in *CYP2C76* and other *CYP2C* genes must be identified and characterized.

Understanding the species difference and the mechanisms behind it is an inevitable task to improve the accuracy in extrapolating the animal data to humans. To accomplish this goal, advancing genomic techniques such as EST or genome

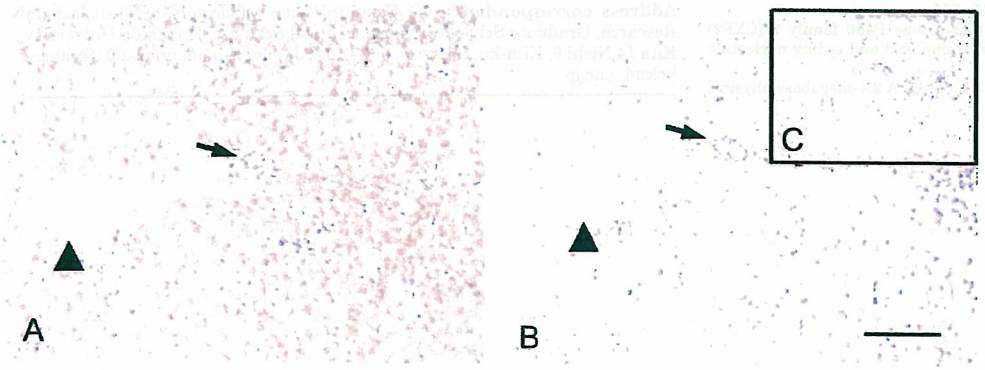

Fig. 7. Immunohistochemical staining of CYP2C76 protein in the liver. Sections were immunostained with anti-CYP2C76 antibodies (A), anti-CYP2C76 antibodies preincubated with blocking peptide (B), or preimmune serum (C). Strong positive staining was observed in hepatocytes, but not in the cells lining the bile duct (arrow) or the vein (arrowhead). Little or no staining was observed after peptide blocking or with preimmune serum. Results are representative of two independent experiments. The magnification is 20× for all pictures. The scale shown by solid line indicates 100 μm.

sequencing, microarray, and comparative genomics should be helpful because they can identify genomic components specific for each animal species including genes, transcripts, and regulatory elements. The ESTs specific for cynomolgus and rhesus monkeys have been identified by our and other groups (Magness et al., 2005), including *CYP2C76*. Further identification and characterization of monkey-specific ESTs will help to better understand the species uniqueness of monkeys in drug metabolism.

In conclusion, we have identified cynomolgus CYP2C76, which does not have the corresponding gene in the human genome. *CYP2C76* contains nine exons and is located in a single *CYP2C* cluster in the monkey genome, similar to the human *CYP2C* genes. Our data show that *CYP2C76* is predominantly expressed in the liver, and its expression level is the greatest among the four *CYP2C* genes analyzed. Moreover, CYP2C76 has a characteristic metabolic profile different from the other CYP2Cs. From these observations, we conclude that cynomolgus CYP2C76 is a major CYP2C contributing substantially to overall drug-metabolizing activity in the liver.

Acknowledgments

We thank the GAIN for providing us invaluable tissue samples from orangutan and chimpanzee, and Ms. Makiko Hase (Applied Biosystems) for assistance in designing gene-specific primers and probes for real-time RT-PCR. We also would like to acknowledge Dr. Aleksandar Milosavljevic at the Baylor College of Medicine for allowing us to access invaluable information on the rhesus monkey genome.

References

Barnes HJ (1996) Maximizing expression of eukaryotic cytochrome P450s in Escherichia coli. *Methods Enzymol* **272:**3–14.

Barnes HJ, Arlotto MP, and Waterman MR (1991) Expression and enzymatic activity of recombinant cytochrome P450 17 alpha-hydroxylase in Escherichia coli. *Proc Natl Acad Sci USA* **88:**5597–5601.

Bellino FL and Wise PM (2003) Nonhuman primate models of menopause workshop. *Biol Reprod* **68:**10–18.

Bogaards JJ, Bertrand M, Jackson P, Oudshoorn MJ, Weaver RJ, van Bladeren PJ, and Walther B (2000) Determining the best animal model for human cytochrome P450 activities: a comparison of mouse, rat, rabbit, dog, micropig, monkey and man. *Xenobiotica* **30:**1131–1152.

Busi F and Cresteil T (2005) CYP3A5 mRNA degradation by nonsense-mediated mRNA decay. *Mol Pharmacol* **68:**808–815.

Christmas P, Jones JP, Patten CJ, Rock DA, Zheng Y, Cheng SM, Weber BM, Carlesso N, Scadden DT, Rettie AE, et al. (2001) Alternative splicing determines the function of CYP4F3 by switching substrate specificity. *J Biol Chem* **276:**38166–38172.

Daigo S, Takahashi Y, Fujieda M, Ariyoshi N, Yamazaki H, Koizumi W, Tanabe S, Saigenji K, Nagayama S, Ikeda K, et al. (2002) A novel mutant allele of the CYP2A6 gene (CYP2A6*11) found in a cancer patient who showed poor metabolic phenotype towards tegafur. *Pharmacogenetics* **12:**299–306.

Fujino H, Yamada I, Shimada S, and Yoneda M (2001) Simultaneous determination of taxol and its metabolites in microsomal samples by a simple thin-layer chromatography radioactivity assay—inhibitory effect of NK-104, a new inhibitor of HMG-CoA reductase. *J Chromatogr B Biomed Sci Appl* **757:**143–150.

Goldstein JA (2001) Clinical relevance of genetic polymorphisms in the human CYP2C subfamily. *Br J Clin Pharmacol* **52:**349–355.

Gotoh O (1992) Substrate recognition sites in cytochrome P450 family 2 (CYP2) proteins inferred from comparative analyses of amino acid and coding nucleotide sequences. *J Biol Chem* **267:**83–90.

Gray IC, Nobile C, Muresu R, Ford S, and Spurr NK (1995) A 2.4-megabase physical map spanning the CYP2C gene cluster on chromosome 10q24. *Genomics* **28:**328–332.

Guengerich FP (1997) Comparisons of catalytic selectivity of cytochrome P450 subfamily enzymes from different species. *Chem Biol Interact* **106:**161–182.

Holbrook JA, Neu-Yilik G, Hentze MW, and Kulozik AE (2004) Nonsense-mediated decay approaches the clinic. *Nat Genet* **36:**801–808.

Iwata H, Fujita K, Kushida H, Suzuki A, Konno Y, Nakamura K, Fujino A, and Kamataki T (1998) High catalytic activity of human cytochrome P450 co-expressed with human NADPH-cytochrome P450 reductase in Escherichia coli. *Biochem Pharmacol* **55:**1315–1325.

Komori M, Kikuchi O, Sakuma T, Funaki J, Kitada M, and Kamataki T (1992) Molecular cloning of monkey liver cytochrome P-450 cDNAs: similarity of the primary sequences to human cytochromes P-450. *Biochim Biophys Acta* **1171:**141–146.

Kuehl P, Zhang J, Lin Y, Lamba J, Assem M, Schuetz J, Watkins PB, Daly A, Wrighton SA, Hall SD, et al. (2001) Sequence diversity in CYP3A promoters and characterization of the genetic basis of polymorphic CYP3A5 expression. *Nat Genet* **27:**383–391.

Kumar S and Hedges SB (1998) A molecular timescale for vertebrate evolution. *Nature (Lond)* **392:**917–920.

Lewis BP, Green RE, and Brenner SE (2003) Evidence for the widespread coupling of alternative splicing and nonsense-mediated mRNA decay in humans. *Proc Natl Acad Sci USA* **100:**189–192.

Ludwig E, Wolfinger H, and Ebner T (1998) Assessment of microsomal tolbutamide hydroxylation by a simple thin-layer chromatography radioactivity assay. *J Chromatogr B Biomed Sci Appl* **707:**347–350.

Magness CL, Fellin PC, Thomas MJ, Korth MJ, Agy MB, Proll SC, Fitzgibbon M, Scherer CA, Miner DG, Katze MG, et al. (2005) Analysis of the *Macaca mulatta* transcriptome and the sequence divergence between Macaca and human. *Genome Biol* **6:**R60.

Matsunaga T, Ohmori S, Ishida M, Sakamoto Y, Nakasa H, and Kitada M (2002) Molecular cloning of monkey CYP2C43 cDNA and expression in yeast. *Drug Metab Pharmacokinet* **17:**117–124.

Narimatsu S, Kobayashi N, Masubuchi Y, Horie T, Kakegawa T, Kobayashi H, Hardwick JP, Gonzalez FJ, Shimada N, Ohmori S, et al. (2000) Species difference in enantioselectivity for the oxidation of propranolol by cytochrome P450 2D enzymes. *Chem Biol Interact* **127:**73–90.

Nelson DR, Koymans L, Kamataki T, Stegeman JJ, Feyereisen R, Waxman DJ, Waterman MR, Gotoh O, Coon MJ, Estabrook RW, et al. (1996) P450 superfamily: update on new sequences, gene mapping, accession numbers and nomenclature. *Pharmacogenetics* **6:**1–42.

Nelson DR, Zeldin DC, Hoffman SM, Maltais LJ, Wain HM, and Nebert DW (2004) Comparison of cytochrome P450 (CYP) genes from the mouse and human genomes, including nomenclature recommendations for genes, pseudogenes and alternative-splice variants. *Pharmacogenetics* **14:**1–18.

Omura T and Sato R (1964) The carbon monoxide-binding pigment of liver microsomes. II. Solubilization, purification and properties. *J Biol Chem* **239:**2379–2385.

Roth GS, Mattison JA, Ottinger MA, Chachich ME, Lane MA, and Ingram DK (2004) Aging in rhesus monkeys: relevance to human health interventions. *Science (Wash DC)* **305:**1423–1426.

Saito T, Takahashi Y, Hashimoto H, and Kamataki T (2001) Novel transcriptional regulation of the human CYP3A7 gene by Sp1 and Sp3 through nuclear factor kappa B-like element. *J Biol Chem* **276:**38010–38022.

Sharer JE, Shipley LA, Vandenbranden MR, Binkley SN, and Wrighton SA (1995) Comparisons of phase I and phase II in vitro hepatic enzyme activities of human, dog, rhesus monkey and cynomolgus monkey. *Drug Metab Dispos* **23:**1231–1241.

Shimada T, Shea JP, and Guengerich FP (1985) A convenient assay for mephenytoin 4-hydroxylase activity of human liver microsomal cytochrome P-450. *Anal Biochem* **147:**174–179.

Stevens JC, Shipley LA, Cashman JR, Vandenbranden M, and Wrighton SA (1993) Comparison of human and rhesus monkey in vitro phase I and phase II hepatic drug metabolism activities. *Drug Metab Dispos* **21:**753–760.

Takagi Y, Takahashi J, Saiki H, Morizane A, Hayashi T, Kishi Y, Fukuda H, Okamoto Y, Koyanagi M, Ideguchi M, et al. (2005) Dopaminergic neurons generated from monkey embryonic stem cells function in a Parkinson primate model. *J Clin Investig* **115:**102–109.

Weaver RJ, Dickins M, and Burke MD (1999) A comparison of basal and induced hepatic microsomal cytochrome P450 monooxygenase activities in the cynomolgus monkey (*Macaca fascicularis*) and man. *Xenobiotica* **29:**467–482.

Address correspondence to: Yasuhiro Uno, Laboratory of Translational Research, Graduate School of Pharmaceutical Sciences, Hokkaido University, Kita 14 Nishi 6, Kita-ku, Sapporo, 060-0812, Japan. E-mail: unoxx001@pharm.hokudai.ac.jp

Cancer Chemother Pharmacol (2006) 58: 494–503
DOI 10.1007/s00280-006-0187-8

ORIGINAL ARTICLE

K. Takasuna · T. Hagiwara · K. Watanabe
S. Onose · S. Yoshida · E. Kumazawa
E. Nagai · T. Kamataki

Optimal antidiarrhea treatment for antitumor agent irinotecan hydrochloride (CPT-11)-induced delayed diarrhea

Received: 3 October 2005 / Accepted: 28 December 2005 / Published online: 25 January 2006

Abstract *Purpose*: An antitumor camptothecin derivative CPT-11 has proven a broad spectrum of solid tumor malignancy, but its severe diarrhea has often limited its more widespread use. We have demonstrated from a rat model that intestinal β-glucuronidase may play a key role in the development of CPT-11-induced delayed diarrhea by the deconjugation of the luminal SN-38 glucuronide, and the elimination of the intestinal microflora by antibiotics or dosing of TJ-14, a Kampo medicine that contains β-glucuronidase inhibitor baicalin, exerted a protective effect. In the present study, we assessed the efficacy of several potential treatments in our rat model to clarify which is the most promising treatment for CPT-11-induced delayed diarrhea. *Methods and results*: Oral dosing (twice daily from days −1 to 4) of streptomycin 20 mg/kg and penicillin 10 mg/kg (Str/Pen), neomycin 20 mg/kg and bacitracin 10 mg/kg (Neo/Bac), both of which inhibited almost completely the fecal β-glucuronidase activity, or TJ-14 1,000 mg/kg improved the decrease in body weight and the delayed diarrhea symptoms induced by CPT-11 (60 mg/kg i.v. from days 1 to 4) to a similar extent. The efficacy was less but significant in activated charcoal (1,000 mg/kg p.o. twice daily from days −1 to 4). In a separate experiment using rats bearing breast cancer (Walker 256-TC), TJ-14, Neo/Bac, and charcoal at the same dose regimen improved CPT-11-induced intestinal toxicity without reducing CPT-11's antitumor activity. In contrast, oral dosing (twice a day) of cyclosporin A (50 mg/kg), a P-glycoprotein and cMOAT/MRP2 inhibitor or valproic acid (200 mg/kg), a UDP-glucuronosyltranferase inhibitor, exacerbated the intestinal toxicity without modifying CPT-11's antitumor activity. *Conclusions*: The result clearly demonstrated the ability of Neo/Bac, Str/Pen, and TJ-14, less but significant ability of activated charcoal, to ameliorate CPT-11-induced delayed-onset diarrhea, suggesting the treatments decreasing the exposure of the intestines to the luminal SN-38 are valuable for improvement of CPT-11-induced intestinal toxicity. In contrast, the treatments affecting the biliary excretion of CPT-11 and its metabolites might have undesirable results.

Keywords CPT-11 · Irinotecan · Diarrhea · β-Glucuronidase

K. Takasuna (✉) · T. Hagiwara · K. Watanabe · S. Onose
New Product Research Laboratories II,
Daiichi Pharmaceutical Co., Ltd.,
16-13 Kita-kasai 1-chome,
Edogawa-ku, 134-8630 Tokyo, Japan
E-mail: takas0p3@daiichipharm.co.jp
Tel.: +81-3-56969080
Fax: +81-3-56968718

S. Yoshida · E. Kumazawa
New Product Research Laboratories III,
Daiichi Pharmaceutical Co., Ltd.,
16-13 Kita-kasai 1-chome,
Edogawa-ku, 134-8630 Tokyo, Japan

E. Nagai
International Marketing Department,
Medical Communications Group,
Daiichi Pharmaceutical Co., Ltd.,
16-13 Kita-kasai 1-chome, Edogawa-ku,
134-8630 Tokyo, Japan

T. Kamataki
Division of Drug Metabolisms,
Faculty of Pharmaceutical Sciences, Hokkaido University,
Kita-12, Nishi-6, Kita-ku, 060 Sapporo, Japan

Introduction

Irinotecan hydrochloride (CPT-11), a water-soluble semisynthetic derivative of camptothecin, is an inhibitor of DNA topoisomerase I enzyme by its main active metabolite SN-38 [1, 2], and a promising antitumor agent, approved worldwide for use in patients with advanced colorectal cancer [3, 4], lung cancer [5, 6], and malignant lymphoma [7]. One of the major dose-limiting toxicities of CPT-11 therapy is unpredictable and severe diarrhea, especially delayed-onset severe diarrhea [inci-

dence of National Cancer Institute (NCI) grade 3 or 4 diarrhea is 20–40%] [8, 9]. It has limited the further evaluation of more aggressive antitumor regimens using CPT-11 [4, 5, 7, 10]. The great interpatient variations in the severity of diarrhea, the pharmacokinetics [11–16], and the efficacy of conventional antidiarrhea agents [5, 17, 18] make it difficult to understand the mechanisms of CPT-11-induced diarrhea, although preclinical and clinical studies have yielded some critical insight into the mechanisms and advances in treatment of the CPT-11-induced side effects [9].

CPT-11 is hydrolyzed by carboxylesterase to form the active metabolite SN-38 [19]. SN-38 is further conjugated to an inactive glucuronic acid conjugate (SN-38 glucuronide) by UDP-glucuronosyltransferase UGT1A1, the same isoenzyme responsible for glucuronidation of bilirubin, and excreted into the bile with other major component CPT-11 and SN-38 by P-glycoprotein (P-gp) and canalicular multispecific organic anion transporter/multidrug resistance-associated protein 2 (cMOAT/MRP2) [20–24]. SN-38 glucuronide may be deconjugated by β-glucuronidase produced by the intestinal microflora, releasing SN-38. The SN-38 deconjugated may largely be responsible for the accumulation of SN-38 in the intestine [25–27].

We have first demonstrated from a rat model that β-glucuronidase produced by microflora in the large intestine may play a key role in the development of CPT-11-induced delayed-onset diarrhea by the deconjugation of the SN-38 glucuronide, and administration of antibiotics exerted a protective effect against the diarrhea by completely inhibiting the β-glucuronidase activity, thereby decreasing the exposure of the large intestine to the luminal SN-38 [28, 29]. Furthermore, we reported that TJ-14 or TJ-114, a Chinese herbal medicine that contains β-glucuronidase inhibitor baicalin, also exerted a protective effect on the delayed-onset diarrhea in the same model [30].

Based on our findings, several nonclinical and clinical studies to alleviate CPT-11-induced diarrhea have been performed especially focusing on the attenuating antiproliferating activity of SN-38 excreted into the intestinal lumen via the bile acid. Up to date, various attractive, and promising treatments for attenuating CPT-11-induced diarrhea, including (1) inhibition of intestinal β-glucuronidase using Kampo medicine TJ-14 [31] or other antibiotics neomycin or bacitracin [32, 33], (2) prevention of intestinal transport (re-absorption) of SN-38 and/or CPT-11 by oral alkalization [34, 35] or by adsorbing of these compounds using activated charcoal [36, 37], or various nonspecific treatments for cancer chemotherapy-induced diarrhea [9], have been clinically demonstrated. However, since these studies were performed under different experimental conditions with each other, no one can expect which is the most promising and effective treatment for CPT-11-induced delayed diarrhea.

To address the question, we compared the antidiarrhea activity of the several potential treatments on CPT-11-induced diarrhea in our rat model.

Methods

Reagents

CPT-11 (Topotecin® Injection, Yakult Honsha, Tokyo, Japan); penicillin G, streptomycin, and valproic acid (Sigma, St Louis, MO, USA); neomycin, bacitracin, and cyclosporin A (Wako Pure Chemicals, Tokyo, Japan); activated charcoal (Iwaki Seiyaku, Tokyo, Japan); and TJ-14 (Hange-Shasin-To, Tsumura, Tokyo, Japan) were commercially purchased. All the potential antidiarrhea agents were dissolved and/or suspended in distilled water for oral administration (Fuso Pharmaceutical Industries, Osaka, Japan) as a volume of 10 or 20 ml/kg.

RPMI1640 medium (Invitrogen Corp.; Carlsbad, CA, USA) and fetal bovine serum (FBS; Hyclone Laboratories Inc.; Logan, UT, USA) were also commercially purchased.

Animals

The experiment was conducted using male Wistar rats (Japan SLC, Hamamatsu, Japan) weighing about 150–180 g ($n=4$–5). The animal room was maintained at a temperature of 23±2°C and a relative humidity of 55±15% with a 12-h light–dark cycle. A commercial animal chow (F-2, Funabashi Farms, Funabashi, Japan) and tap water were freely available throughout the acclimatization and experimental periods.

Experimental schedule

Animals were intravenously administered CPT-11 (60 mg/kg) from the tail vein once a day (a.m.) for four consecutive days (from days 1 to 4). In the following three antibiotic groups, 2 mg streptomycin and 1 mg penicillin, 2 mg neomycin, or 2 mg neomycin per ml of drinking water was administered from 5 days before the start of CPT-11 administration and throughout the experiment (days −5 to 4), respectively, to aspire complete individual antibiotic efficacy. Antibiotics (Str/Pen, streptomycin 20 mg/kg and penicillin 10 mg/kg; Neo, neomycin 20 mg/kg; Neo/Bac, neomycin 20 mg/kg and bacitracin 10 mg/kg), TJ-14 (1,000 mg/kg), or activated charcoal (1,000 mg/kg) were orally administered twice a day (a.m. and p.m.) from the day before (day −1) to 4 days after the start of CPT-11 injection. Under the CPT-11's regimen adopted [60 mg/kg i.v. once daily for consecutive 4 days (days 1–4)], the diarrhea monitored throughout days 5–8 was similar to human diarrhea in terms of being resistant to conventional antidiarrhea agents [38]. Diarrhea, the onset which was on or after day 5, was defined delayed diarrhea. The severity of delayed diarrhea and the daily body weight were monitored, and the results were used as an index of intestinal toxicity. The severity of delayed diarrhea was scored as follows:

- Normal (0, normal stool)
- Slight (1, slightly wet stool without staining of the coat)
- Moderate (2, wet and unformed stool with moderate perianal staining of the coat)
- Severe (3, watery stool with severe staining of the coat around the anus)

The total diarrhea score area under the score-day curve during days 5–9, and the mean score at each day were calculated. Watery diarrhea which appeared within about 2 h after the administration of CPT-11 was defined acute diarrhea. Before the start of CPT-11 administration on day 1, the fecal β-glucuronidase activity was determined by a modification of the procedure of Akao et al. [39], and the fecal pH using pH meter (HM-50G, Toa Electrics, Tokyo, Japan) after homogenization of the samples in 0.9% physiological saline.

In a separate experiment, the effects of several potential antidiarrhea treatments on CPT-11-induced antitumor activity and diarrhea were evaluated using rats bearing breast cancer. The rat breast cancer cell line Walker 256-TC cells were obtained from Cell Resource Center for Biomedical Research, Tohoku University (Miyagi, Japan) and were cultured in vitro in RPMI1640 medium supplemented with 10% (v/v) fetal bovine serum. The cultures were grown at 37°C in a 5% CO_2–95% air atmosphere, and the passages were performed twice a week. The Walker 256-TC cells (1×10^5 cells/0.1 ml) were inoculated subcutaneously into the right flank of rats. When the mean estimated tumor volume reached about 300 mm^3 on day 7 after tumor inoculation, the rats were randomly divided into experimental groups (five rats per group) to have the similar mean estimated tumor volume, and were given CPT-11 at the same regimen mentioned above with the following potential antidiarrhea compounds. (1) TJ-14 1,000 mg/kg, (2) activated charcoal 1,000 mg/kg, (3) Neo/Bac, neomycin 20 mg/kg and bacitracin 10 mg/kg—these three treatments showed an obvious antidiarrhea activity in the normal rats in the present study, (4) cyclosporin A 50 mg/kg, (5) valproic acid 200 mg/kg. Both cyclosporine A and valproic acid had been expected to enhance CPT-11's antitumor activity with reduced intestinal toxicity because both increase the area under plasma concentration–time curve of SN-38 by lowering biliary excretion of SN-38 or by inhibiting SN-38 conjugation. All these compounds were orally administered twice daily (a.m. and p.m.) for days −1 to 4, except that Neo/Bac group received 2 mg neomycin per ml of drinking water from 5 days before the start of CPT-11 administration. The estimated tumor volume was measured 4, 7, and 10 days after the start of CPT-11 administration, and the severity of delayed diarrhea and the daily body weight were also monitored.

The estimated tumor volume was calculated using the formula:

$$\text{The estimated tumor volume } (mm^3) = \frac{L \times W^2}{2},$$

where L and W represent the length and the width of the tumor mass, respectively.

All experimental procedures were performed in accordance with the in-house guidelines of the Institutional Animal Care and Use Committee of Daiichi Pharmaceutical Co., Ltd.

Results

Fecal pH and β-glucuronidase activity in normal rats

On day 1 (6 days after the start of antibiotics administration), the fecal pH and β-glucuronidase activity in the control group were 6.42 and about 190 nmol/min/mg protein, respectively. The fecal pH in the treatment groups was similar to that in the control group, except for Str/Pen group in which the fecal pH was 7.20. The fecal β-glucuronidase activities in Str/Pen and Neo/Bac treated groups were reduced to less than approximately 10% of the control group. The fecal β-glucuronidase activity of Neo group was also reduced but it remained in about 20% of the control group. The fecal β-glucuronidase activities in TJ-14 and activated charcoal groups had somewhat higher values as compared with that of the control group but it was not a statistically significant change (Fig. 1).

Effects on CPT-11-induced body weight loss and diarrhea symptoms in normal rats

Following the i.v. administration of CPT-11 (60 mg/kg once daily for the consecutive 4 days: days 1–4), body weight decreased from day 2 and reached a nadir on day 8, being about 23% decrease as compared with the initial value (day 1). No diarrhea was present during the first 2 days, but acute watery diarrhea occurred on days 3 and 4 within 1–2 h after CPT-11 injection. Thereafter, diarrhea was chronically present during days 5–8 (delayed diarrhea).

Each treatment had little or no effect on CPT-11-induced decrease in body weight during days 2–3. On or after day 4, either treatment inhibited the decrease in body weight, and improved the delayed diarrhea symptoms. Str/Pen, Neo, Neo/Bac, and activated charcoal, but not TJ-14, also inhibited the acute watery diarrhea that appeared on days 3 and 4. There was an obvious difference of the effectiveness among the treatments. In consideration of the changes of body weight and diarrhea score, the rank order for beneficial effect on CPT-11-induced intestinal toxicity was Str/Pen = TJ-14 = Neo/Bac > activated charcoal > Neo (Figs. 2, 3).

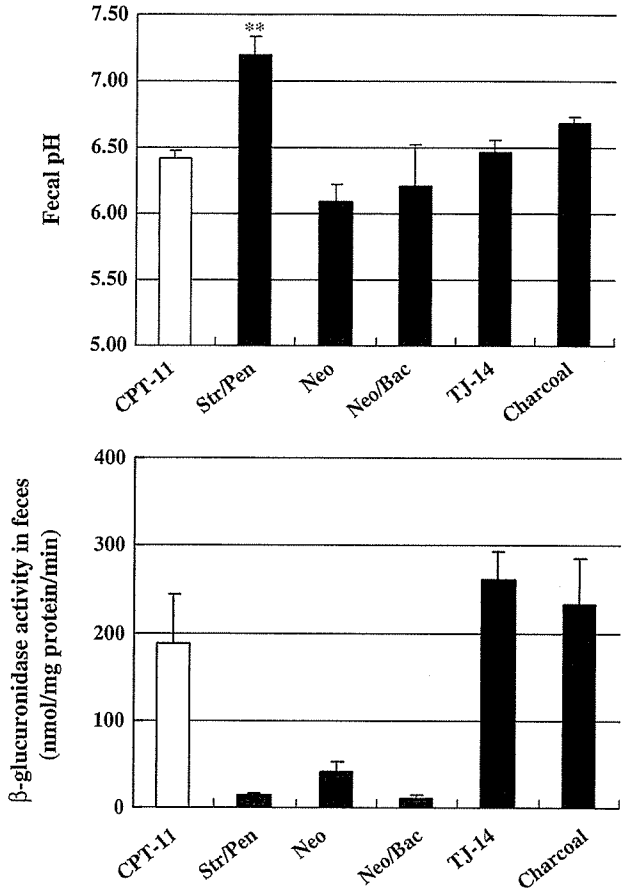

Fig. 1 The pH and β-glucuronidase activity of the feces on the day (day 1) of the start of CPT-11 (60 mg/kg, once daily for 4 days) injection in normal rats. Antibiotics, except for bacitracin, were administered in drinking water from 5 days (day −5) before the start of CPT-11 injection. Each data represents the mean of 4–5 animals. $^{**}P<0.01$ versus CPT-11 group (Dunnett test). *Str/Pen* streptomycin (2 mg/ml) and penicillin (1 mg/ml) in drinking water + streptomycin 20 mg/kg and penicillin 10 mg/kg p.o.; *Neo* neomycin (2 mg/ml) in drinking water + neomycin 20 mg/kg p.o.; *Neo/Bac* neomycin (2 mg/ml) in drinking water + neomycin 20 mg/kg and bacitracin 10 mg/kg p.o.; *TJ-14* TJ-14 1,000 mg/kg p.o. *Charcoal* activated charcoal 1,000 mg/kg p.o

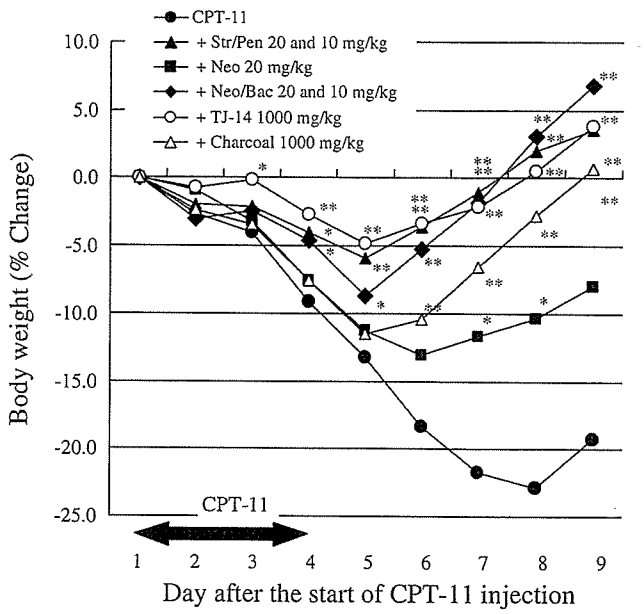

Fig. 2 Effects of several agents on CPT-11-induced body weight loss in rats. CPT-11 was given intravenously at a dose of 60 mg/kg once daily for four consecutive days (days 1–4). The agents were orally administered twice daily from the day before to 4 days after the start of CPT-11 injection. In addition, antibiotics, except for bacitracin, were administered in drinking water from 5 days before to 4 days after the start of CPT-11 injection. The change in body weight was calculated on the basis of that on day 1. Each point represents the mean of 4–5 animals. The abbreviations are referred in Fig. 1. $^{*}P<0.05$, $^{**}P<0.01$ versus CPT-11 group (Dunnett test)

Effects on CPT-11-induced antitumor activity and intestinal toxicity (body weight loss and diarrhea symptoms) in rats bearing breast cancer

The mean estimated tumor volume in the vehicle control group increased linearly and reached about 10,000 mm^3, which was approximately 30-fold its initial mean estimated tumor volume of 300 mm^3, on day 10. CPT-11 (60 mg/kg once daily for the consecutive 4 days: days 1–4) showed moderate but significant reduction of the mean estimated tumor volume on days 4 and 7, but its antitumor effect was no longer apparent (not significant) on day 10. The body weight decreased from day 2 and reached a nadir on day 6, being about 15% decrease as compared with the initial value (day 1). No diarrhea was present during the first 2 days, but acute watery diarrhea

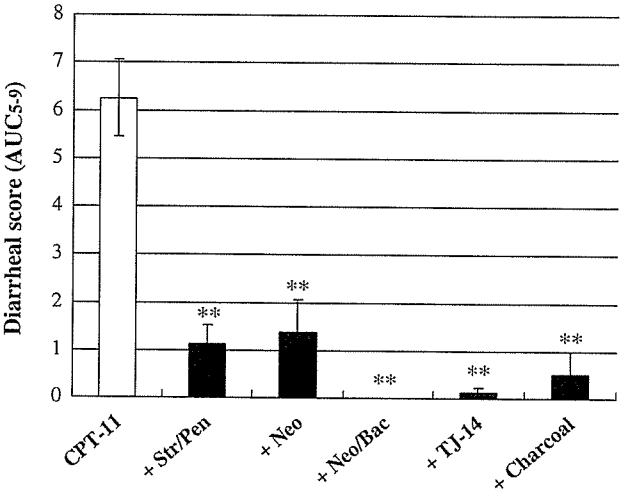

Fig. 3 Effects of several agents on CPT-11 (60 mg/kg i.v., once daily for 4 days)-induced delayed diarrhea symptoms in rats. The agents were orally administered twice daily from the day before to 4 days after the start of CPT-11 injection. In addition, antibiotics, except for bacitracin, were administered in drinking water from 5 days before to 4 days after the start of CPT-11 injection. Each data represents the mean of 4–5 animals. The abbreviations are referred in Fig. 1. $^{**}P<0.01$ versus CPT-11 (Wilcoxon rank sum test)

occurred on days 3 and 4 within 1–2 h after CPT-11 injection. Thereafter, diarrhea was chronically present during days 6–7 (delayed diarrhea).

TJ-14, Neo/Bac, and activated charcoal inhibited the decrease in body weight, and improved the delayed diarrhea, but had no effect on the antitumor effect of CPT-11. Neo/Bac, but not TJ-14 or activated charcoal, also inhibited the acute watery diarrhea that appeared on days 3 and 4. In contrast, cyclosporin A and valproic acid augmented the loss of body weight gain and delayed diarrhea symptom score while those had no effects on CPT-11's antitumor activity (Figs. 4, 5). In addition, the acute diarrhea appeared not only on days 3 and 4 but also on day 1 in cyclosporin A and valproic acid groups.

Discussion

The clinical use of CPT-11 has been associated with early onset diarrhea that is observed immediately after CPT-11 injection (acute diarrhea) and delayed-onset diarrhea that occurs more than 24 h after CPT-11 injection and usually continues for several days (delayed diarrhea) [9, 10]. The former was usually accompanied with cholinergic symptoms such as salivation, cramps, and diaphoresis, and could be controlled with cholinergic receptor blocker atropine [40]. Therefore, its anticholinesterase activity [41, 42] is at least involved in the cholinergic symptoms including acute diarrhea. Indeed, we have confirmed that CPT-11 has not only anti-acetylcholinesterase activity but also anti-butyrylcholinesterase activity which plays a major role in the intestinal tract (unpublished data).

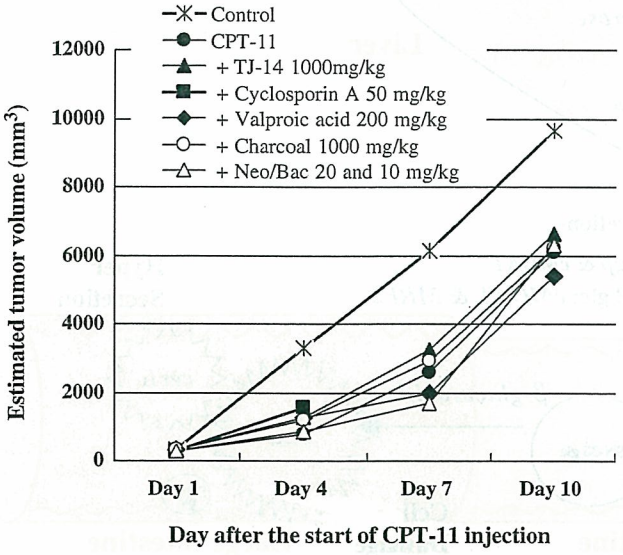

Fig. 4 Effects of several agents on antitumor activity of CPT-11 (60 mg/kg iv for 4 days) in rats bearing breast cancer (Walker 256-TC). The agents were orally administered twice daily from the day prior to the start of CPT-11 injection for total of 5 days. In addition, neomycin was administered in drinking water from 5 days prior to the start of CPT-11 injection for total of 9 days. All rats died until day 7 in cyclosporin A-treated group. One rat died on day 8 in valproic acid-treated group. *TJ-14* TJ-14 1,000 mg/kg, p.o.; *cyclosporin A* cyclosporin A 50 mg/kg, p.o.; *valproic acid* valproic acid 200 mg/kg, p.o.; *charcoal* activated charcoal 1,000 mg/kg, p.o.; *Neo/Bac* neomycin (2 mg/ml) in drinking water + neomycin 20 mg/kg and bacitracin 10 mg/kg, p.o. Each value represents the mean of 2–5 animals. There are no significant differences of the estimated tumor volumes between the CPT-11 alone and CPT-11 with agents on days 4, 7, or 10 (Student's *t* test)

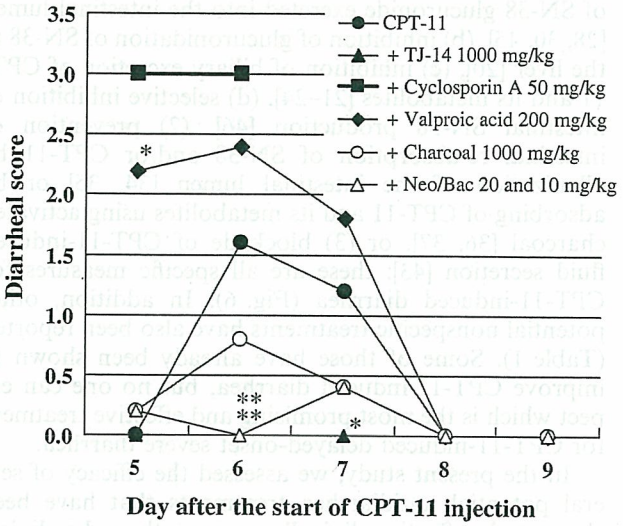

Fig. 5 Effects of several agents on delayed diarrhea symptoms caused by CPT-11 (60 mg/kg iv for 4 days) in rats bearing breast cancer (Walker 256-TC). The agents were orally administered twice daily from the day prior to the start of CPT-11 injection for total of 5 days. In addition, neomycin was administered in drinking water from 5 days prior to the start of CPT-11 injection for total of 9 days. All rats died until day 7 in cyclosporin A-treated group. One rat died on day 8 in valproic acid-treated group. The abbreviations are referred in Fig. 4. Each value represents the mean of 2–5 animals. $*P < 0.05$, $**P < 0.01$: Significantly different from the group treated with CPT-11 alone (Wilcoxon rank sum test)

In contrast, the latter is unexpected diarrhea, the severe [National Cancer Institute-Common Toxicity Criteria (NCI-CTC) grade 3 or 4] diarrhea might be a potentially life-threatening disorder, especially when concomitant with severe neutropenia. Although many pharmacokinetic analysis in humans have been made to predict the incidence or the mechanisms of delayed diarrhea, there are somewhat conflicting results [11–16]. Namely, there are no generally accepted relationship between the severity of diarrhea and any of the studied pharmacokinetic parameters.

Intensive loperamide regimens have been considered as the standard antidiarrhea treatment for CPT-11-induced diarrhea in Europe and the United States. It is one of the nonspecific treatments for cancer chemotherapy-induced diarrhea and probably reduces diarrhea by delaying intestinal transit allowing increased time for fluid absorption or reducing the fluid secretion [43], but the clinical studies could not necessarily confirm its satisfied efficacy [44]. Other potential approaches are (1) altering the metabolism [(a) inhibition of deconjugation

of SN-38 glucuronide excreted into the intestinal lumen [28, 30, 45], (b) inhibition of glucuronidation of SN-38 in the liver [20], (c) inhibition of biliary excretion of CPT-11 and its metabolites [21–24], (d) selective inhibition of intestinal SN-38 production [46], (2) prevention of intestinal re-absorption of SN-38 and/or CPT-11 by alkalization of the intestinal lumen [34, 35] or by adsorbing of CPT-11 and its metabolites using activated charcoal [36, 37], or (3) blockade of CPT-11-induced fluid secretion [43]: these are all specific measures for CPT-11-induced diarrhea (Fig. 6). In addition, other potential nonspecific treatments have also been reported (Table 1). Some of those have already been shown to improve CPT-11-induced diarrhea, but no one can expect which is the most promising and effective treatment for CPT-11-induced delayed-onset severe diarrhea.

In the present study, we assessed the efficacy of several potential antidiarrhea treatments that have been shown to be effective clinically or currently under clinical trial, in comparison with those of Str/Pen or TJ-14 treatment that has been confirmed effective in our rat model [28, 30]. The present result was well in agreement with our previous reports, namely both Str/Pen and

Table 1 Summary of nonspecific approaches and other potential approaches to prevent CPT-11-induced diarrhea

Nonspecific measures
Enkephalinase inhibitor (Tiorphan) [51]
COX_2 inhibitor (Celecoxib) [52]
IL-15 [53]
Sandostatin [44, 54, 55]
Lipopeptide JBT-3002 [56, 57]
RDP58 [58]
Radical scavenger (amifostine) [59]
Sucralfate and nifuroxazide [60]
Thalidomide [61, 62]
Glutamate [63]
Steroid (budesonide) [64]
Fish oil [65]
Modified schedule of CPT-11 dosing [66–68]
Pharmacogenetic analysis of UDP-glucuronosyltransferase [69]

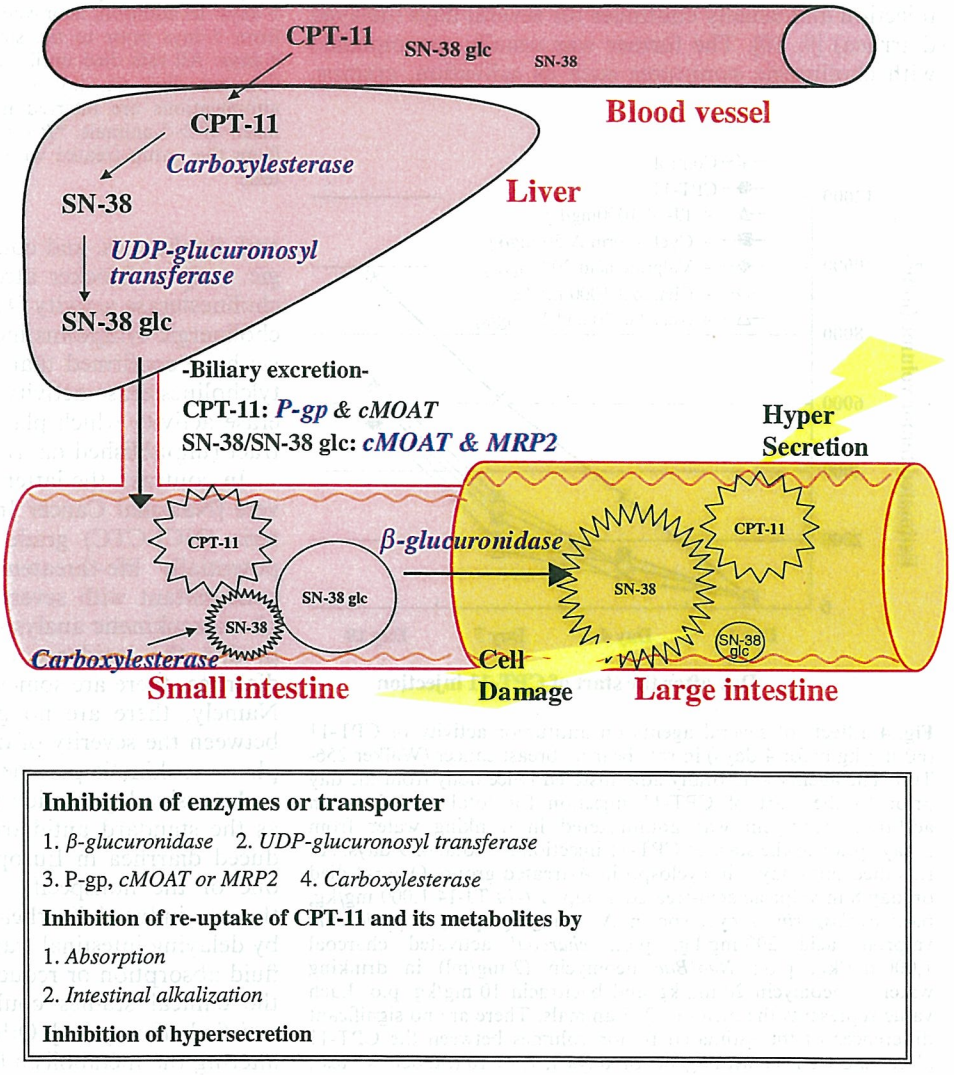

Fig. 6 Schematic representation of CPT-11 metabolism, expecting CPT-11-specific approaches to prevent intestinal toxicity of CPT-11

TJ-14 showed good antidiarrhea activity against CPT-11-induced delayed diarrhea, and first revealed that their efficacy was almost equivalent. The other poorly absorbed aminoglycoside antibiotics Neo/Bac also showed good antidiarrhea activity similar to that of Str/Pen or TJ-14. In contrast, the efficacy of single co-administration of neomycin was relatively low as compared with the above three treatment regimens despite inhibition (about 80%) of intestinal β-glucuronidase activity. The possible reason why neomycin could not ameliorate the CPT-11-induced intestinal toxicity as other two antibiotic regimens might be due to an incomplete inhibition of β-glucuronidase activity (< 80% in Neo vs. > 90% in Str/Pen or Neo/Bac). Another possible reason might be due to the change of fecal pH. Takeda et al. [34] and Ikegami et al. [35] have recently reported that intestinal alkalization by sodium bicarbonate supplementation ameliorated CPT-11-induced diarrhea with reduction of the histopathological damage to the mucosa of the intestine by influencing the conversion of SN-38/CPT-11 from lactone to carboxylate. In the present study, the fecal pH in Str/Pen group changed to be about pH 7.2 from the pH 6.4 (control group). The respective rates of intestinal uptake for CPT-11 and SN-38 were shown to be pH sensitive, with uptake decreasing by more than 65% at pH levels greater than 6.8 [47], suggesting that intestinal alkalization by Str/Pen might, at least in part, be involved in the ameliorating mechanism while the reason of the change in pH is not known. Since, however, there is no change in the fecal pH of Neo/Bac or TJ-14 group which exerted efficacy comparable to Str/Pen, alkalization in the intestinal lumen might not play a key role in the ameliorating efficacy of these treatments used in the present study.

An alternative measure for the inhibition of β-glucuronidase in the intestinal lumen is pharmacological inhibition using specific inhibitors including natural glucuronides [48]. Indeed, we have reported that TJ-14 or TJ-114 (0.5 and 1 g/kg twice daily), a Chinese herbal medicine that contains β-glucuronidase inhibitor baicalin, or baicalin itself (25 mg/kg) exerted a protective effect on the delayed-onset diarrhea in rats [30]. D-Glucaric acid-1,4-lactone monohydrate, a specific β-glucuronidase inhibitor, has recently been shown to reduce CPT-11-induced mucosal damage in the small intestine in rats [45]. Our preliminary study, however, did not confirm its antidiarrhea activity. The dose of glucaro-1,4-lactone used in the preliminary study (25 mg/kg orally twice daily) might be enough to inhibit β-glucuronidase because it has β-glucuronidase inhibitory activity comparable to baicalin [48]. The reason why glucaro-1,4-lactone had no efficacy in our rat model remains to be determined. We reported that CPT-11-induced delayed-onset diarrhea would be attributable to the damage to the cecum, which has the highest β-glucuronidase activity in the luminal contents, and the inhibition of β-glucuronidase by antibiotics resulted in mainly the reduction of the cecal damage, not of the small intestine [28]. Since Fittkau et al. [45] reported that glucaro-1,4-lactone reduced CPT-11-induced mucosal damage in the small intestine which almost lacks β-glucuronidase activity in the luminal contents [28], other mechanisms apart from β-glucuronidase inhibition in the intestinal lumen might be involved. Alternatively, the therapeutic effect of Kampo medicine TJ-14 on CPT-11-induced delayed diarrhea might be solely based on the inhibition of SN-38 glucuronide deconjugation but also on other mechanisms including a suppression prostaglandin E_2 production in the colon [49].

Chowbay et al. [50] reported that activated charcoal was not effective in the prevention of CPT-11-induced diarrhea as compared with inhibition of β-glucuronidase in the intestinal microflora by ceftriaxone, a third generation cephalosporin. In the present study, activated charcoal showed clearly improved CPT-11-induced intestinal toxicity though its activity was slightly weak as compared with Str/Pen, Neo/Bac, or TJ-14. Therefore, the adsorption of CPT-11 and its metabolites using activated charcoal could offer some help in reducing CPT-11-induced diarrhea as reported by Michael et al. [36] and Maeda et al. [37].

Although the pharmacokinetic or histopathologic examinations were not conducted in the present study, we have shown good correlation between the severity of indices of intestinal toxicity adopted in this study and histopathological changes in the intestine [28, 30]. Moreover, the inhibition of β-glucuronidase in the intestinal microflora by antibiotics [29, 50] or TJ-14 (unpublished data) did not affect SN-38 or CPT-11 plasma pharmacokinetics. It is suggested that the antibiotics or TJ-14 could prevent CPT-11-induced intestinal toxicity without reducing antitumor activity. Indeed, antibiotics (Neo/Bac), TJ-14, or activated charcoal ameliorated CPT-11-induced intestinal toxicity with maintenance of CPT-11's antitumor activity in rats bearing breast cancer in the present study. Since the biliary excretion of CPT-11, its active metabolite SN-38 and SN-38 glucuronide are mediated by the P-gp and cMOAT/MRP2 in the bile canalicular membrane [20–24], inhibition of the transporters, or UDP-glucuronosyl transferase has been proposed to reduce the intestinal toxicity of CPT-11 by decreasing the biliary excretion of particularly SN-38 and SN-38 glucuronide or potentially increase the CPT-11 therapeutic index by decreasing the intestinal toxicity associated with more aggressive antitumor regimens. In the present study, contrary to ones expectations, cMOAT/MRP2 inhibitor cyclosporin A or UDP-glucuronosyl transferase inhibitor valproic acid exacerbated the intestinal toxicity, and did not modify CPT-11's antitumor activity. As we do not confirm whether or not CPT-11 can show dose-dependent antitumor activity in the present rat model bearing breast cancer, we cannot conclude that co-administration of cyclosporin A or valproic acid does not enhance CPT-11's antitumor activity from the present study. However, the fact that cyclosporin A and valproic acid caused a worsening intestinal toxicity, and may produce adverse systemic reaction, probably keeping SN-38 serum and

tissue levels too high [20, 21, 23], is suggesting that it is at risk of potentiating the systemic and/or intestinal side effect of CPT-11 to control biliary excretion of CPT-11 and its metabolites by drugs for preventing CPT-11-induced intestinal toxicity in consideration of individual difference of biliary pharmacokinetics.

The present results conclude that the optimal combined use of antibiotics which completely reduces the intestinal, bacterial β-glucuronidase activity prevents CPT-11-induced intestinal toxicity to a similar extent of Kampo medicine TJ-14, and activated charcoal, a more inexpensive agent, may also be useful when antibiotics or TJ-14 could induce severe secondary complications. Moreover, the treatments affecting the biliary excretion of CPT-11 and its metabolites might have undesirable results.

To date, a lot of CPT-11 specific and nonspecific (Fig. 6, Table 1) antidiarrhea treatment designs have been proposed in animal and human studies. However, to our knowledge only Kampo medicine and antibiotics could improve CPT-11-induced delayed-onset diarrhea in both animal and human studies although our rat model might be different from human in terms of types of intestinal microflora and anatomical distribution. Therefore, we currently think that Kampo medicine, antibiotics, or both treatments if possible, are the optimal antidiarrhea treatments against CPT-11-induced diarrhea.

References

1. Kunimoto T, Nitta K, Tanaka T, Uehara N, Baba H, Takeuchi M, Yokokura T, Sawada S, Miyasaka T, Mutai M (1987) Antitumor activity of 7-ethyl-10-[4-(1-piperidino)-1-piperidino]carbonyloxy-camptothecin, a novel water-soluble derivative of camptothecin, against murine tumors. Cancer Res 47:5944–5947
2. Kawato Y, Aonuma M, Hirota Y, Kuga H, Sato K (1991) Intracellular roles of SN-38, a metabolite of the camptothecin derivative CPT-11, in the antitumor effect of CPT-11. Cancer Res 51:4187–4191
3. Rothenberg ML, Kuhn JG, Burris III HA, Nelson J, Eckardt JR, Tristan-Morales M, Hilsenbeck SG, Weiss GR, Smith LS, Rodriguez GI, Rock MK, VonHoff DD (1993) Phase I and pharmacokinetic trial of weekly CPT-11. J Clin Oncol 11:2194–2204
4. Shimada Y, Yoshino M, Wakui A, Nakao I, Futatsuki K, Sakata Y, Kambe M, Taguchi T, Ogawa N (1993) Phase II study of CPT-11, a new camptothecin derivative, in metastatic colorectal cancer. J Clin Oncol 11:909–913
5. Fukuoka M, Niitani H, Suzuki A, Motomiya M, Hasegawa K, Nishiwaki Y, Kuriyama T, Ariyoshi Y, Negoro S, Masuda N, Nakajima S, Taguchi T (1992) A phase II study of CPT-11, a new derivative of camptothecin, for previously untreated non-small-cell lung cancer. J Clin Oncol 10:16–20
6. Noda K, Nishiwaki Y, Kawahara M, Negoro S, Sugiura T, Yokohama A, Fukuoka M, Mori K, Watanabe K, Tamura T, Yamamoto S, Saijo N (2002) Irinnoteacn plus cisplatin compared with etoposide plus cisplatin for extensive small-cell-lung cancer. N Engl J Med 346:85–91
7. Ohno R, Okada K, Masaoka T, Kuramoto A, Arima T, Yoshida Y, Ariyoshi H, Ichimaru M, Sakai Y, Oguro M, Ito Y, Morishima Y, Yokomaku S, Ota K (1990) An early phase II study of CPT-11: a new derivative of camptothecin, for the treatment of leukemia and lymphoma. J Clin Oncol 8:1907–1912
8. Sargent DJ, Niedzwiechi D, O'Connell MJ, Schilsky RL (2001) Recommendation for caution with irinotecan, fluorouracil, and leucovorin for colorectal cancer. N Engl J Med 345:144–145
9. Hecht JR (1998) Gastrointestinal toxicity of irinotecan. Oncology 12(8 Suppl 6):72–78
10. Saliba F, Hagipantelli R, Misset JL, Bastian G, Vassal G, Bonnay M, Herait P, Cote C, Mahjoubi M, Mignard D, Cvitkovic E (1998) Pathophysiology and therapy of irinotecan-induced delayed-onset diarrhea in patients with advanced colorectal cancer: a prospective assessment. J Clin Oncol 16:2745–2751
11. Ohe Y, Sakai Y, Shinkai T, Eguchi K, Tamura T, Kojima A, Kunikane H, Okamoto H, Karato A, Ohmatsu H, Kanzawa F, Saijo N (1993) Phase I study and pharmacokinetics of CPT-11 with 5-day continuous infusion. J Natl Cancer Inst 84:972–974
12. Kudoh S, Fukuoka M, Masuda N, Kusunoki Y, Matsui K, Negoro S, Takifuji N, Nakagawa K, Hirashima T, Tamanoi M, Nitta T, Yana H, Takada M (1993) Relationship between CPT-11 pharmacokinetics and diarrhea in the combination chemotherapy of irinotecan (CPT-11) and cisplatin (CDDP). Proc Am Soc Clin Oncol 12:141
13. Gupta E, Lestingi TM, Mick R, Ramirez J, Vokes EE, Ratain MJ (1994) Metabolic fate of irinotecan in humans: correlation of glucuronidation with diarrhea. Cancer Res 54:3723–3725
14. Catimel G, Chabot GG, Guastalla JP, Dumortier A, Cote C, Engel C (1995) Phase I and pharmacokinetic study of irinotecan (CPT-11) administered daily for three consecutive days every three weeks in patients with advanced solid tumors. Ann Oncol 6:133–140
15. Chabot GG, Abigerges D, Catimel G, Culine S, DeForni M, Extra JM (1995) Population pharmacokinetics and pharmacodynamics of irinotecan (CPT-11) and active metabolite SN-38 during phase I trials. Ann Oncol 6:141–151
16. Xie R, Mathijssen RHJ, Sparreboom A, Verweij J, Karlsson MO (2002) Clinical pharmacokinetics of irinotecan and its metabolites in relation with diarrhea. Clin Pharmacol Ther 72:265–275
17. Masuda N, Fukuoka M, Kudoh S, Kusunoki Y, Matsui K, Takifuji N, Nakazawa K, Tamanoi M, Nitta T, Hirashima T, Negoro S, Takada M (1993) Phase I and pharmacologic study of irinotecan in combination with cisplatin for advanced lung cancer. Br J Cancer 68:777–782
18. Abigerges D, Armand JP, Chabot GG, DaCosta L, Fadel E, Cote C, Hérait P, Gandia D (1994) Irinotecan (CPT-11) high-dose escalation using intensive high-dose loperamide to control diarrhea. J Natl Cancer Inst 86:446–449
19. Rivory LP, Bowels MR, Robert J, Pond SM (1996) Conversion of irinotecan (CPT-11) to its active metabolite, 7-ethyl-10-hydroxycamptothecin (SN-38), by human liver carboxylesterase. Biochem Pharmacol 52:1103–1111
20. Gupta E, Wang X, Ramirez J (1997) Modulation of glucuronidation of SN-38, the active metabolite of irinotecan, by valproic acid and phenobarbital. Cancer Chemother Pharmacol 39:4440–4444
21. Gupta E, Safa AR, Wang X (1996) Pharmacokinetic modulation of irinotecan and metabolites by cyclosporin. Cancer Res 56:1309–1314
22. Horikawa M, Kato Y, Tyson CA, Sugiyama Y (2002) The potential for an interaction between MRP2 (ABCC2) and various therapeutic agents: probenecid as a candidate inhibitor of the biliary excretion of irinotecan metabolites. Drug Metab Pharmacokinet 17:23–33
23. Arimori K, Kuroki N, Hidaka M, Iwakiri T, Yamasaki K, Okumura M, Ono H, Takamura N, Kikuchi M, Nakano M (2003) Effect of p-glycoprotein modulator, cyclosporin A, on the gastrointestinal excretion of irinotecan and its metabolite SN-38 in rats. Pharm Res 20:910–917
24. Itoh T, Itagaki S, Sasaki K, Hirano T, Takemoto I, Iseki K (2004) Pharmacokinetic modulation of irinotecan metabolites by sulphobromophthalein in rats. J Pharm Pharmacol 56:809–812
25. Kaneda N, Yokokura T (1990) Nonlinear pharmacokinetics of CPT-11 in rats. Cancer Res 50:1721–172

26. Atsumi R, Suzuki W, Hakusui H (1991) Identification of the metabolites of irinotecan, a new derivative of camptothecin, in rat bile and its biliary excretion. Xenobiotica 21:1159–1169
27. Kuhn JG (1998) Pharmacology of irinotecan. Oncology 12(8 Suppl 6):39–42
28. Takasuna K, Hagiwara T, Hirohashi M, Kato M, Nomura M, Nagai E, Yokoi T, Kamataki T (1996) Involvement of beta-glucuronidase in intestinal microflora in the intestinal toxicity of the antitumor camptothecin derivative irinotecan hydrochloride (CPT-11) in rats. Cancer Res 56:3752–3757
29. Takasuna K, Hagiwara T, Hirohashi M, Kato M, Nomura M, Nagai E, Yokoi T, Kamataki T (1998) Inhibition of intestinal microflora beta-glucuronidase modifies the distribution of the active metabolite of the antitumor agent, irinotecan hydrochloride (CPT-11) in rats. Cancer Chemother Pharmacol 42:280–286
30. Takasuna K, Kasai Y, Kitano Y, Mori K, Kobayashi R, Hagiwara T, Kakihata K, Hirohashi M, Nomura M, Nagai E, Kamataki T (1995) Protective effects of kampo medicines and baicalin against intestinal toxicity of a new anticancer camptothecin derivative, irinotecan hydrochloride (CPT-11), in rats. Jpn J Cancer Res 86:978–984
31. Mori K, Kondo T, Kamiyama Y, Kano Y, Tominaga K (2003) Preventive effect of Kampo medicine (Hangeshashin-to) against irinotecan-induced diarrhea in advanced non-small-cell lung cancer. Cancer Chemother Pharmacol 51:403–406
32. Kehrer DF, Sparreboom A, Verweij J, DeBruijn P, Nierop CA, Van de Schraaf J, Ruijgrok EJ, DeJonge MJ (2001) Modulation of irinotecan-induced diarrhea by cotreatment with neomycin in cancer patients. Clin Cancer Res 7:1136–1141
33. Alimonti A, Satta F, Pavese I, Burattini E, Zoffoli V, Vecchione A (2003) Prevention of irinotecan plus 5-fluorouracil/leucovorin-induced diarrhoea by oral administration of neomycin plus bacitracin in first-line treatment of advanced colorectal cancer. Ann Oncol 14:805–806
34. Takeda Y, Kobayashi K, Akiyama Y, Soma T, Handa S, Kudoh S, Kudoh K (2001) Prevention of irinotecan (CPT-11)-induced diarrhea by oral alkalization combined with control of defecation in cancer patients. Int J Cancer 92:269–275
35. Ikegami T, Ha L, Arimori K, Latham P, Kobayashi K, Ceryak S, Matsuzaki Y, Bouscarel B (2002) Intestinal alkalization as a possible preventive mechanism in irinotecan (CPT-11)-induced diarrhea. Cancer Res 62:179–187
36. Michael M, Brittain M, Nagai J, Feld R, Hedley D, Oza A, Siu M, Moore J (2001) A phase II study of activated charcoal to prevent irinotecan (CPT-11) induced diarrhea (abstract). Proc Am Soc Clin Oncol 1615
37. Maeda Y, Ohune T, Nakamura M, Yamasaki M, Kiribayashi Y, Murakami T (2004) Prevention of irinotecan-induced diarrhoea by oral carbonaceous adsorbent (Kremezin™) in cancer patients. Oncol Rep 12:581–585
38. Takasuna K, KasaiY, Kitano Y, Mori K, Kakihata K, Hirohashi M, Nomura M (1995) Study on the mechanisms of diarrhea induced by a new anticancer camptothecin derivative, irinotecan hydrochloride (CPT-11), in rats (in Japanese). Folia Pharmacol Jpn 105:447–460
39. Akao T, Akao T, Kobayashi K (1987) Glycyrrhizin β-D-glucuronidase of *Eubacterium* sp from human intestinal flora. Chem Pharm Bull 35:705–710
40. Gandia D, Abigerges D, Armand JP (1993) CPT-11-induced cholinergic effects in cancer patients (letter). J Clin Oncol 11:196–197
41. Kawato Y, Sekiguchi M, Akahane K, Tsutomi Y, Hirota Y, Kuga H, Suzuki W, Hakusui H, Sato K (1993) Inhibitory activity of camptothecin derivatives against acetylcholinesterase in dogs and their binding activity to acetylcholine receptors in rats. J Pharm Pharmacol 45:444–448
42. Morton CL, Wadkins RM, Danks MK, Potter PM (1999) The anticancer prodrug CPT-11 is a potent inhibitor of acetylcholinesterase but is rapidly catalyzed to SN-38 by butyrylcholinesterase. Cancer Res 59:1458–1463
43. Suzuki T, Sakai H, Ikari A, Takeguchi N (2000) Inhibition of thromboxane A(2)-induced Cl(−) secretion by antidiarrhea drug loperamide in isolated rat colon. J Pharmacol Exp Ther 295:233–238
44. Barbounis V, Koumakis G, Vassilomanolakis M, Demiri M, Efremidis AP (2001) Control of irinotecan-induced diarrhea by octreotide after loperamide failure. Support Care Cancer 9:258–260
45. Fittkau M, Vogit W, Holzhausen HJ, Schmoll HJ (2004) Saccharic acid 1,4-lactone protects against CPT-11-induced mucosa damage in rats. J Cancer Res Clin Oncol 130:388–394
46. Wadkins RM, Hyatt JL, Yoon KJP, Morton CL, Lee RE, Damodaran K, Beroza P, Danks MK, Potter PM (2004) Discovery of novel selective inhibitors of human intestinal carboxylesterase for the amelioration of irinotecan-induced diarrhea: synthesis, quantitative structure–activity relationship analysis, and biological activity. J Pharmacol Exp Ther 65:1336–1343
47. Kobayashi K, Bouscarel B, Matsuzaki Y, Ceryak S, Kudoh S, Fromm H (1999) pH-dependent uptake of irinotecan and its active metabolite, SN-38, by intestinal cells. Int J Cancer 83:491–496
48. Narita M, Nagai E, Hagiwara H, Aburada M, Yokoi T, Kamataki T (1993) Inhibition of β-glucuronidase by natural glucuronides of Kampo medicines using glucuronide of SN-38 (7-ethyl-10-hydroxycamptothecin) as a substrate. Xenobiotica 21:5–10
49. Kase Y, Hayakawa T, Aburada M, Komatsu Y, Kamataki T (1997) Preventive effects of Hange-shashin-to on irinotecan hydrochloride-caused diarrhea and its relevance to the colonic prostaglandin E_2 and water absorption in the rat. Jpn J Pharmacol 75:407–413
50. Chowbay B, Sharma A, Zhou QU, Cheung YB, Lee ED (2003) The modulation of irinotecan-induced diarrhea and pharmacokinetics by three different classes of pharmacologic agents. Oncol Rep 10:745–775
51. Goncalves E, DeCosta L, Abigerges D, Armand JP (1995) A new enkephalinase inhibitor as an alternative to loperamide in the prevention of diarrhea induced by CPT-11. J Clin Oncol 13:2144–2146
52. Trifan OC, Durham WF, Salazar VS, Horton J, Levine BD, Zweifel BS, Davis TW, Masferrer JL (2002) Cyclooxygenase-2 inhibition with celecoxib enhances antitumor efficacy and reduces diarrhea side effect of CPT-11. Cancer Res 15:5778–5784
53. Cao S, Black JD, Troutt AB, Rustum YM (1998) Interleukin 15 offers selective protection from irinotecan-induced intestinal toxicity in a preclinical animal model. Cancer Res 58:3270–3274
54. Pro B, Lozano R, Ajani JA (2001) Therapeutic response to octreotide in patients with refractory CPT-11 induced diarrhea. Invest New Drugs 19:341–343
55. Zidan J, Haim N, Beny A, Stein M, Gez E, Kuten A (2001) Octreotide in the treatment of severe chemotherapy-induced diarrhea. Ann Oncol 12:227–229
56. Shinohara H, Killion JJ, Kuniyasu H, Kumar R, Fidler IJ (1998) Prevention of intestinal toxic effect and intensification of irinotecan's therapeutic efficacy against murine colon cancer liver metastases by oral administration of the lipopeptide JBT-3002. Clin Cancer Res 4:2053–2063
57. Shinohara H, Killion JJ, Bucana CD, Yano S, Fidler IJ (1999) Oral administration of the immunomodulator JBT-3002 induces endogenous interleukin 15 in intestinal macrophages for protection against irinotecan-mediated destruction of intestinal epithelium. Clin Cancer Res 5:2148–2156
58. Zhao J, Huang L, Belmar N, Buelow R, Fong T (2004) Oral RDP58 allows CPT-11 dose intensification for enhanced tumor response by decreasing gastrointestinal toxicity. Clin Cancer Res15:2851–2859
59. Delioukina ML, Prager D, Parson M, Hecht JR, Rosen P, Rosen LS (2002) Phase II trial of irinotecan in combination with amifostine in patients with advanced colorectal carcinoma. Cancer 94:2174–2179

60. Duffour J, Gourgou S, Seitz JF, Senesse P, Boutet O, Castera D, Kramar A, Ychou M (2002) Efficacy of prophyractic antidiarrhoeal treatment in patients receiving Campto for advanced colorectal cancer. Anticancer Res 22:3727–3732
61. Govindarajan R, Heaton KM, Broadwater R, Zeitlin A, Lang NP, Hauer-Jensen M (2000) Effect of thalidomide on gastrointestinal toxic effects of irinotecan. Lancet 356:566–567
62. Tchekmedyian NS (2002) Thalidomide and irinotecan-associated diarrhea. Am J Clin Oncol 25:324
63. Savarese D, Al-Zoubi A, Boucher J (2000) Glutamine for irinotecan diarrhea. J Clin Oncol 18:450–451
64. Lenfers BHM, Loeffler TM, Droege CM, Hausamen TU (1999) Substantial activity of budesonide in patients with irinotecan (CPT-11) and 5-fluorouracil induced diarrhea and failure of loperamide treatment. Ann Oncol 10:1251–1253
65. Hardman WE, Moyer MP, Cameron IL (1999) Fish oil supplementation enhanced CPT-11 (irinotecan) efficacy against MCF7 breast carcinoma xenografts and ameliorated intestinal side-effects. Br J Cancer 81:440–448
66. Kurita A, Kado S, Kaneda N, Onoue M, Hashimoto S, Yokokura T (2000) Modified irinotecan hydrochloride (CPT-11) administration schedule improves induction of delayed-onset diarrhea in rats. Cancer Chemother Pharmacol 46:211–220
67. Fujii H, Koshiyama M, Konishi M, Yoshida M, Tauchi K (2002) Intermittent, repetitive administrations of irinotecan (CPT-11) reduces its side-effects. Cancer Detect Prev 26:210–212
68. Kurita A, Kado S, Kaneda N, Onoue M, Hashimoto S, Yokokura T (2003) Alleviation of side effects induced by irinotecan hydrochloride (CPT-11) in rats by intravenous infusion. Cancer Chemother Pharmacol 52:349–360
69. Ando Y, Saka H, Ando M, Sawa T, Muro K, Ueoka H, Yokoyama A, Saitoh S, Shimokata K, Hasegawa Y (2000) Polymorphism of UDP-glucuronosyltranferase gene and irinotecan toxicity: a pharmacogenetic analysis. Cancer Res 60:6921–6926

BIOPHARMACEUTICS & DRUG DISPOSITION
Biopharm. Drug Dispos. 27: 353–359 (2006)
Published online in Wiley InterScience
(www.interscience.wiley.com) **DOI:** 10.1002/bdd.518

Comparative *Cytochrome P450 -1A1, -2A6, -2B6, -2C, -2D6, -2E1, -3A5* and *-4B1* Expressions in Human Larynx Tissue Analysed at mRNA Level

Devrim Sarikaya[a], Cem Bilgen[b], Tetsuya Kamataki[c] and Zeki Topcu[d,*]
[a] *Department of Bioengineering, Faculty of Engineering, Ege University, Izmir, 35100 Turkey*
[b] *Department of Otorhinolaryngology, Faculty of Medicine, Ege University, Izmir, 35100 Turkey*
[c] *Laboratory of Drug Metabolism, Graduate School of Pharmaceutical Sciences, Hokkaido University, Sapporo 060-0812, Japan*
[d] *Department of Pharmaceutical Biotechnology, Faculty of Pharmacy, Ege University, Izmir, 35100 Turkey*

ABSTRACT: The metabolic activation of numerous exogenous and endogenous chemicals is catalysed by cytochrome P450 enzymes (CYPs). The aim of this study was to analyse the expression of the individual forms of CYP at the mRNA level in human larynx and quantitatively to compare their expressions in human liver, the main organ of CYP expression. Individual forms of CYP mRNAs were detected by reverse transcriptase-polymerase chain reaction (RT-PCR) using specific primers for the *CYPs -1A1, -1A2, -2A6, -2B6, -2C, -2D6, -2E1, -3A3/4, -3A5, -3A7* and *-4B1*. An RNA competitor of known copy number, covering the primer sequences necessary to amplify the entire object *CYPs* within a single molecule, was used as reference. This study reports a consistent detection of mRNAs for the *CYPs -1A1, -2A6, -2B6, -2C, -2D6, -2E1, -3A5* and *-4B1* in the human larynx tissue. The data indicate that the human larynx highly resembles the lung tissue in CYP content, as a comparable subset of CYP mRNAs was detected in the larynx previously reported for human lung with the exception of *CYP1A2*. The results are discussed in quantitative ratios of the detected CYP mRNAs in relation to the hepatic CYP expression. Copyright © 2006 John Wiley & Sons, Ltd.

Key words: cytochrome P450; laryngeal tissue; drug metabolizing enzymes

Introduction

Cytochrome P450 (CYP) (E.C. 1.14.14.1) is a heme-containing enzyme responsible for the metabolism of numerous endogenous and exogenous compounds [1]. Approximately 20 individual CYPs have been identified in man [1,2]. The regulation of *CYP* expression is, in part, tissue-specific leading to a tissue-selective response for a given xenobiotic compound. The majority of *CYP* genes are expressed most abundantly in the liver, yet many *CYPs* were also reported in extrahepatic tissues [3]. Relatively little is known about the individual CYP forms present in the human larynx. The larynx forms a connection from the pharynx to the trachea and it has histological resemblances to the nasal mucosa, trachea and lung, which are formed by a set of hyaline and elastic cartilages in a complex muscular architecture [4]. Its function is to maintain patency of the passage to prevent swallowed food or liquid from entering the trachea in a valve-like manner. Being a tissue with a high exposure to both inhaled and blood-borne xenobiotic compounds, the larynx is an important target for cancer, which makes it a

*Correspondence to: Department of Pharmaceutical Biotechnology, Faculty of Pharmacy, Ege University, Izmir, 35100 Turkey.
E-mail: zeki.topcu@ege.edu.tr

Received 27 January 2006
Revised 31 May 2006
Accepted 6 June 2006